UNLIMITED DISTRIBUTION

National Defence
Research and Development Branch

Défense nationale
Bureau de recherche et développement

TECHNICAL MEMORANDUM 88/204
February 1988

FLOW VISUALIZATION EXPERIMENTS WITH SUBMARINE MODELS IN A WIND TUNNEL

Michael Mackay

Defence Research Establishment Atlantic

Centre de Recherches pour la Défense Atlantique

Canada

UNLIMITED DISTRIBUTION

National Defence
Research and Development Branch

Défense nationale
Bureau de recherche et développement

FLOW VISUALIZATION EXPERIMENTS WITH SUBMARINE MODELS IN A WIND TUNNEL

Michael Mackay

February 1988

Approved by L.J. Leggat Director/Technology Division

DISTRIBUTION APPROVED BY

D/TD

TECHNICAL MEMORANDUM 88/204

Defence Research Establishment Atlantic

Centre de Recherches pour la Défense Atlantique

Canada

ABSTRACT

Flow visualization experiments were carried out in the NAE 2 x 3 m low speed wind tunnel with some members of a systematic series of idealized submarine configurations. Only hull-alone and hull and sail configurations were tested. The experiments were done at Reynolds numbers between 4.9 and 9.5 million.

Results are reported for hull flow separation, flow on the sail and for flow in the sail/hull junction. In addition to some derived quantitative data, many photographs and interpretive sketches are included.

Résumé

Des expériences de visualisation de l'écoulement ont été menées à basse vitesse sur des éléments structuraux de systèmes de configurations idéales de sous-marins dans la soufflerie de 2 x 3 de l'EAN. Des modèles avec coque seulement et avec coque et kiosque ont fait l'objet d'essais. Les expériences ont été exécutées avec des nombres de Reynolds compris entre 4,9 et 9,5 millions.

Des résultats ont été consignées pour la séparation de l'écoulement sur la coque, de l'écoulement sur le kiosque et de l'écoulement à la jonction coque-kiosque. En plus de certaines valeurs quantitatives dérivées, le présent document contient de nombreuses photos ainsi que des croquis explicatifs.

TABLE OF CONTENTS

NOMENCLATURE

$\overline{A}$	Attachment line (on flow sketches)
D	Maximum hull diameter
F	Focus (on flow sketches)
L	Hull length: 1778 mm
N	Node (on flow sketches)
R_e	Reynolds number based on hull length and freestream flow velocity
S	Saddle point (on flow sketches)
$\overline{S}$	Separation line (on flow sketches)
S*	Shear stress line (on flow sketches)
V	Vortex (on flow sketches)
x	Longitudinal axis, normally expressed as a station number, from 0 at the nose to 10 at the tail
y	Offset of the nose profile in the horizontal plane, nondimensionalized by D
z	Offset of the nose profile in the vertical plane, nondimensionalized by D
α	Pitch angle; also angle of incidence for the axisymmetric hull alone
β	Yaw angle
ϕ_s	Angular location of hull separation relative to the crossflow direction

1. INTRODUCTION

DREA is studying the manoeuverability and general hydrodynamics of submarines. A major part of this work involves model testing in a number of facilities including wind tunnels and towing tanks. Fundamental to the experimental program will be the comparison of results for a systematic series of idealized submarine forms in the different facilities; this will also provide a database for future analytical developments.

To establish the physical aspects of the flow and to assist with interpreting the experimental measurements, it is necessary to do flow visualization. A previous document[1] has described initial experiments in the small National Aeronautical Establishment (NAE) water tunnel. This memorandum will describe the results of flow visualization for some members of the systematic series, using larger, 1778 mm, models in the NAE 2 x 3 m low speed wind tunnel. The experiments consisted of flow visualization on the surface of the model using the oil/pigment (or paint) technique.

The scope of this memorandum is limited to presenting the results of these experiments, and making some general observations on the nature of the flowfield. The principal features of the method will be outlined (Section 3) in sufficient depth for a reader unfamiliar with the technique to understand the interpretations which follow.

Results are presented for two hull-alone configurations and for three hull and sail configurations. Both pitch and yaw were varied, and a small number of runs were made to evaluate the effect of Reynolds number.

2. EXPERIMENTAL DESCRIPTION

2.1 Wind Tunnel

These experiments were done in the NAE 2 x 3 m low speed wind tunnel. Actual dimensions of the working section are 6 ft high by 9 ft wide with corner fillets containing lighting fixtures. Physically, the basic tunnel is little altered from the early description of Wardlaw[2], but the instrumentation and data acquisition systems have been continually modernized in recent years.

The models were cantilevered from the tunnel sting mount as shown in Figure 1. As oriented in the photograph, the model rotates in yaw with the turntable in the floor of the tunnel. To introduce a component of pitch, the model is rotated about its own axis. The fairing on the vertical sting support rotates counter to the turntable so that it remains aligned with the freestream flow.

2.2 Models

The models comprised one tail/midbody unit, two interchangable nose units and two interchangable sails. The former was constructed of GRP over high density foam on a 7075 aluminum spine. Hard points were provided to attach the nose units and sails which were all made of laminated wood. As shown in Figure 1(b), station markings from 0 at the most forward point of the nose to 10 at the tip of the tail (truncated for the sting attachment) were provided. The models were manufactured by Eastern Marine Services Ltd, Musquodoboit Harbour, N.S.

Changing nose units gave two alternative hull configurations, axisymmetric or asymmetric. Both hulls were 1778 mm long (L) and had a slenderness ratio (L/D) of 8.75. The principal dimensions and geometry of the model are given below.

Tail:
- 3D long
- axisymmetric,
- parabolic longitudinal section profile,
- truncated and faired at about station 9.5 for the sting mount, Figure 1(b).

Midbody:
- 4D long,
- axisymmetric, with constant radius D/2.

Axisymmetric Nose:
- L/5 long,
- longitudinal section defined by a Riegels[3] D_2 profile with 3 x NACA standard nose radius.

Asymmetric Nose:
- L/5 long,
- longitudinal section in the horizontal plane (y) defined by a Riegels[3] D_2 profile with 3 x NACA standard nose radius.
- longitudinal section in the vertical plane (z) defined by a transformation of the horizontal profile according to:

$$z = 0.5\ (2y)^{0.1} \qquad (1)$$

- elliptical transverse cross-sections.

The two sails were identical in planform but different in thickness. Sail F was the same as used in the water tunnel[1], while sail S had more prototypical proportions:

Sail F:
- (3/2)D chordlength,
- (6/7)D height (span),
- NACA 0028.6 section,
- leading edge located at 0.3L.

Sail S:
- (3/2)D chordlength,
- (6/7)D height (span),
- NACA 0020 section,
- leading edge located at 0.3L.

The principal dimensions of the models are sketched in Figure 2, and the asymmetric nose, showing a number of cross-sections, is sketched in Figure 3. The configuration made up of the axisymmetric hull with sail S is the parent form of the idealized systematic series.

2.3 Procedures

The conventional oil flow visualization technique was applied in these experiments; a short discussion of how to interpret the results is given in the next section. The oil/pigment mixture used was arrived at after trial and error since previous tests at NAE have generally used white pigment on black models (as in Reference 4, for example), rather than a dark pigment on a white model. The mixture was principally lampblack in vacuum oil, with small amounts of titanium dioxide and oleic acid added to achieve a good compromise between granularity and dispersal of the pigment[5]. The mixture was brushed on to the model. With vacuum oil, evaporation of the mixture during the runs was negligable.

The principal test Reynolds number was 7 million (tunnel speed 56 m/s), with a limited amount of data taken at Reynolds numbers of 4.9 and 9.5 million (tunnel speeds 40 and 77 m/s respectively). The tunnel speed was limited by model vibration at the higher angles of yaw. To stimulate transition to turbulent flow, a band of #80 grit was applied at about 3 percent of hull length on the axisymmetric nose, about 2 percent on the asymmetric nose, and over the first 2 percent of the sails.

Photographs were taken both from outside the tunnel while it was running and from inside the tunnel after it was turned off. Run times were between 10 and 20 minutes depending upon how fast the pattern was developing. Since the models were oriented differently for each run, it was not practical to use fixed camera positions; hand-held cameras were used, concentrating on the most interesting features of each pattern. This approach, although flexible and quite fast, did not permit a high degree of quantitative accuracy in the observations. To obtain such accuracy, considerably more sophisticated and time-consuming photogrammetric techniques would have had to be employed.

Table I lists the conditions for each experimental test series. Positive pitch is with the nose up with respect to the freestream flow; the sign of yaw is arbitrary.

3. VISUALIZATION OF LIMITING STREAMLINES

Oil flow visualization creates an image of the shear stress pattern on the surface. Most important, the direction of the stress vector is the limiting streamline of the flow close to the surface. In practice, this correspondance is slightly modified by the stress induced in the oil film, but long experience with different oils and pigments has produced combinations which will give reliable indications over most of a given flow. The definitive analysis of this technique is given by Squire et al[5].

During the run, the pattern can be seen developing, and is considered to be fully developed, or run to completion, when no significant further changes can be observed. Ideally, at this point, the oil should be mostly evaporated from or blown off the model, so that the pattern can be observed at leisure with the tunnel turned off. This can never be the case for a complex model such as used here, since oil will accumulate in low stress (near stagnant flow) regions, and will run under the influence of gravity on non-horizontal surfaces. This last effect is present even during the run, and will introduce a gravitational bias to the pattern as noted in some of the following sections.

While the technique can be adjusted to counteract some of the difficulties outlined above, compromises must be made when several aspects of the flow are to be observed. For example, lines of attachment are generally clearer in an underdeveloped pattern, axial separation lines (ie: those directed approximately along the flow direction) can generally be observed consistently without special precautions, and for lateral separations the pattern should be run further towards completion.

Convergence of the limiting streamlines indicates flow separation at a line or a singular point, examples of which are shown in Figures 4 and 5. The corresponding patterns with flow direction reversed indicate attachment. Real flows will typically show a complex combination of these singularities; many examples are given in References 4,7 and 8. In this report, the following nomenclature is used in sketches of the flow:

$\overline{S}$ - line of separation,
$\overline{A}$ - line of attachment,
N - node on the surface,
F - focus on the surface,
S - saddle point on the surface or in the crossflow field, and
V - vortex in the crossflow field.

Topological rules for flow on the surface and in the field have been formulated by Hunt et al in Reference 8. This reference specifically treats the flow around bluff obstacles, such as submarine sails.

When only limiting streamline information is available, the interpretation of flow in the field is difficult and often ambiguous. This is illustrated in Figure 6 for the common observation of two separation lines (on each side) along a circular cylinder at incidence. The simplest interpretation, 6(b), has the lower separation line as the "primary separation" and the source of the predominant vortex, with a single induced (secondary) vortex, whereas the alternative interpretation, 6(c), formed by the addition of a saddle point and an additional secondary vortex, also obeys the topological rules, but no longer associates the predominant vortex with either separation line. Direct observation of flow in the field is required to determine which flow pattern is correct. This is typically a very time-consuming experimen , since a high resolution of the field is required. Some good examples of this, showing measurement of the flowfield about a prolate spheroid using a ten-hole pressure probe, are given by Meier et al[9].

Aside from the reservations noted above with regard to separation location in some cases, lines of separation are generally well delineated by the oil flow technique since flow convergence causes a concentration of the pigment along the line. Conversely, attachment lines, where the flow diverges, are often difficult to observe, particularly in a pattern run towards completion.

Dickinson[10] has presented some oil flow patterns around an appendage-like obstacle. He introduces the term "shear stress line" for the demarcation between areas of low and high stress. The appearance of these areas is characterized in Reference 5 as, low stress: heavy in oil and pigment with slowly movin' transverse wavelets, and high stress: a scoured surface with marked granular streaking. The examples shown by Dickinson indicate very sharp shear stress lines. These can be readily confused with separation lines, and vice-versa. As sketched in Figure 7, the shear stress and separation lines can be considered to be stages in the evolution of a secondary flow. This process could apply equally well to a body flow pattern as to the corner flow shown. The thickness of the oil/pigment film is exaggerated in the figure, but in flows of this type, where large build-ups may occur, there is always a possibility that interactions are modifying the pattern. The observations discussed below showed a number of examples of possible shear stress lines; these are indicated by S* in the sketches.

4. RESULTS

4.1 Axisymmetric Hull Alone

The model sting mount arrangements precluded useful observations aft of station 9. No afterbody separation was observed in tests at zero incidence; this was consistent with a calculation of the turbulent boundary layer, using Truckenbrodt's method[11], which predicted that separation would occur aft of station 9.3. Some asymmetric tail separation was seen with the model at incidence, but oil build-up and the tail modifications cast doubt on the reliability of these observations.

A hull at incidence exhibits the classic crossflow separation with leeward body vortices. Figure 8 shows a well-developed pattern for the axisymmetric hull at 12 degrees incidence; the photograph was taken with the tunnel off, therefore the lines are running slightly. The lower line of the pattern is clearly a separation line (in conventional interpretation, the primary separation line); the upper one may be a shear stress line. At incidences of 16 and 20 degrees the upper line appeared to be a true separation. The leeward attachment line coincides with the numbers on the model.

At incidence, the gravitational bias noted in the previous section increased ϕ_s, the angular location of separation, on the upper half of the hull, and reduced it on the lower. Average values of ϕ_s are shown in Figures 9, 10 and 11. Neither run at 4 or 8 degrees clearly indicated body separation, and data at 16 degrees were uncertain at the forward stations due to glare. In these, and following estimates of separation, resolution of the model grid and uncertainty of the camera angle limited absolute estimates of ϕ_s to within about ±5 degrees. The trends shown in Figure 9 for the primary separation line are consistent with those previously observed in the water tunnel[1]: ϕ_s decreases and the longitudinal start of separation moves forward with increasing incidence. The apparent start of separation was in a relatively stagnant region which did not show good detail.

Figure 11 suggests that the longitudinal start of separation moved forward with increasing Reynolds number; a trend for ϕ_s is not so clear. Estimates of ϕ_s from the water tunnel experiments (at Reynolds numbers of about 4×10^4, corresponding to laminar, rather than turbulent flow) were between 115 and 125 degrees on the midsection.

The results in Figures 9 and 11 agree qualitatively with axisymmetric body data compiled by Spangler et al in Reference 12. The most notable difference was that the longitudinal start of separation in the present experiments was further forward than would be expected from the other data; this is illustrated by Figure 12. Spangler's data is for missile noses, typically ogive profiles, which may explain the discrepancy.

4.2 Asymmetric Hull Alone

In discussing body separation from the asymmetric hull, it is first necessary to consider the influence of forebody flow, Figures 13, 14 and 15. In each case, body separation appears to be initiated far forward by the modified nose profile. Typically, large regions of stagnant flow lie along the forebody separation lines, making determination of the lines difficult. Notably in Figure 14, the pure yaw case, they have more the appearance of shear stress lines.

Estimates of the body separation for the asymmetric hull alone are plotted in Figures 16 to 19. Data for the afterbody are generally not shown on these figures due to excessive oil build-up in this series of tests. The start of the primary separation line was far forward, as already noted, but ϕ_s still decreased with increasing pitch or yaw. For secondary separation, the opposite trend appeared. In all previous cases, only one line has been plotted because of symmetry, but symmetry is lost for this body in simultaneous pitch and yaw, Figure 15. The corresponding estimates of location, Figure 19, show this asymmetry for the forebody, but aft of station 5 the flow was again symmetrical within the resolution of the estimates.

4.3 Sail

Figure 20 demonstrates that there was very little trailing edge separation for sail F in axial flow. Note that flow in this picture is from the left, whereas in those that follow it is from the right. Aft of about 30 percent of chord, separation occurred along the tip edge with reattachment further down the sail and the formation of small tip vortices, Figure 21.

The pattern was qualitatively as above for negative pitch except that the attachment line extended from further forward and was lower on the sail. The sheer stress line near the tip was similarly shifted and looked more like a true secondary separation.

As a yaw angle was introduced, Figures 22 and 23, the separated region moved forward from the trailing edge. At 8 degrees, within the separated region, the influence of gravity lead to a build-up at the root trailing edge. Flow coming around the trailing edge appeared to be inducing a focus-like pattern. At 12 degrees yaw, the separated region extended further forward. The focus-like structure was clearer; it appeared to represent a rotary recirculation within the trailing edge separation bubble.

Increasing yaw to 16 degrees, the root extent of the separation bubble moved all the way to the sail leading edge, but was little changed further up the sail, Figure 24. The rotary recirculation was prominant. This pattern requires a saddle point located approximately as shown, although it was not well defined in the photographs. Development of the separation in a trailing edge stall, as shown in this series of tests, is characteristic of thick foil sections.

The pattern observed for sail S developed as described above up to a yaw angle of 12 degrees, except that the extent of separation was not so large as for sail F; compare Figures 25 and 26 with Figures 22 and 23. On increasing yaw to 16 degrees, a large change was seen in the pattern, with separation originating at the root leading edge and extending up the sail to delimit a bubble-like structure which was reflected in the adjacent hull, Figure 27. The forward moving flow over most of the sail was very close to stagnation, and therefore, for practical purposes, the sail can be considered to be totally stalled at this yaw angle. The model experienced visible buffeting.

Figure 28 shows the pattern for a yaw angle of 16 degrees at the low Reynolds number, 4.9 million. The separated region is much more sharply defined than for observations at a Reynolds number of 7 million (the previous figure), and stall is not so far advanced since flow is shown attached over almost half the sail area. The small region of flow near the root leading edge is also more clearly like a focus singularity. The photographs appear to show a small reflection of this focus on the adjacent part of the hull.

Observations of sail S on the asymmetric hull showed no difference from patterns already presented for sail S on the axisymmetric hull. There was an additional run in this series at a yaw of 20 degrees which is shown in Figure 29. The pattern is a development of the 16 degree yaw case. Most of the principal features are more clearly defined; these include the separation bubble just aft of the leading edge with an extensive region of reversed flow downstream of it, focii near the leading edge and on the hull, a node low on the trailing edge and saddle points on both sail and hull. Figure 30 shows the sail trailing edge node and the hull saddle point in greater detail. At 20 degrees yaw, buffeting of the model was so severe that the tunnel speed was brought very cautiously up to the test Reynolds number.

Sail S on the asymmetric hull was also run with simultaneous pitch and yaw as shown in Figure 31. Qualitatively, the leeward pattern on the sail appeared to be determined by the yaw component, while the pitch component caused a net spanwise displacement of the pattern near the tip. Flow in Figure 31(a) is from the right, and in Figure 31(b), from the left.

4.4 Sail/Hull Junction

A frontal view of the junction flow for sail F on the axisymmetric hull is given in Figure 32; details from the side were shown in Figure 20. Qualitatively, the pattern observed agrees with the interpretation reported by Dickinson[10] for a foil mounted on a flat plate. The line inside the initial separation appears to be a shear

stress line. Further in toward the sail, an attachment line is clear over the forward part of the junction, but is less easy to determine aft. The pattern aft of the sail is dominated by the low stress regions starting near the sail root trailing edge, Figure 33. These regions appear to delineate the path of oil and pigment accumulated in the sail separation region and draining off at the root.

The axial flow case did not reveal enough detail to permit an interpretation of the character of the junction vortex, although the apparent reattachment on the hull suggests that the vortex is quite small and close to the hull, as proposed by Dickinson. The inner, counter-rotating vortex reported by him was not apparent in this case.

The extent of the junction flow region was quite strongly dependent on pitch angle for sail F, but less so for sail S. Estimates of axial location of the $\overline{S}$ and S* lines along the centerline are plotted in Figure 34 (this axial location corresponds to the saddle point for the separation line). Out from the centerline, or longitudinal plane of symmetry, both lines moved proportionally in towards, or away from, the sail. In the case of sail F, the most sensitive to pitch, the extent of junction flow approximately doubled going from a pitch angle of -12 to +12 degrees. For the attachment lines, the trend was opposite: they were close in to the sail at the positive pitch angle and moved away towards the S* line as pitch decreased. The attachment lines appeared to originate from the attachment node at the sail root leading edge.

Examples of junction flow at two yaw angles are shown in Figure 35; the pattern was qualitatively unchanged from that of axial flow, but moved with the shift of streamlines on the hull. Estimates of this movement for the saddle point on the separation line are plotted in Figure 36. Note that, as previously, the angular coordinate is measured from the crossflow direction.

Only one of the junction flow cases clearly suggested an interpretation other than that proposed by Dickinson. This was sail S on the asymmetric hull in simultaneous pitch and yaw ($\alpha = \beta = 8.55$ degrees); the pattern is shown in Figure 37. Limiting streamlines converge on the inner line, identifying it as a separation line rather than a shear stress line. There is also an additional line of attachment between this, and the primary separation line upstream. The presumed flowfields are sketched in Figure 38(a) for the other junction flow cases and in Figure 38(b) for the present case.

The inner attachment line on the leeward side tended to move back in towards the sail root trailing edge, particularly at low yaw angles. At 8 degrees yaw, the primary separation also moved in towards the root trailing edge, so that the vortex appeared to be climbing up the leeward side of the sail, Figure 39.

4.5 Other Sail/Hull Interactions

The flow pattern on the hull was generally underdeveloped for hull/sail configurations since the run time was optimized for details of flow on the sail. Photographic coverage of the effect of the sail on the hull separation lines was therefore incomplete and this section is limited to some qualitative observations on the interaction.

In positive pitch, there appeared to be a merging of the junction flow separation lines with the hull separation lines on the upper part of the afterbody. Adjacent to the sail there was a displacement of the hull separation lines as noted in the water tunnel tests[1]. There were no significant interactions in negative pitch.

In yaw, the formerly observed locations of hull separation occupy upper and lower positions on the hull (see the small sketch on Figure 18). Clearly, the upper line is located to interact strongly with the sail. The upper line was not apparent on the forebody in these experiments, but appeared as an extension of the windward side separation line, directed aft close to the centerline of the afterbody, regardless of yaw angle. The lower hull separation line did not appear to be significantly affected by the sail. For example, in the photograph and sketch of Figure 40, the values of ϕ_s for the lower line appear to be close to those plotted for the hull alone, in Figure 18. Another view of this test, from a somewhat higher angle, was given in Figure 29.

5. CONCLUDING REMARKS

The surface flow visualization experiments described in this memorandum were undertaken to provide background information for DREA experimental work in submarine hydrodynamics. Where possible, quantitative results have been presented, although without considerably increasing the sophistication of the method of observation, the degree of accuracy is limited.

The difficulties of interpreting the observed patterns have been outlined. It was noted that there was often a degree of organization within an apparently separated region.

Parameters investigated included pitch, yaw and Reynolds number. A reasonable number of observations were made for hull separation, mostly for the hull-alone configurations, and for flow on the sail. A good level of detail was obtained for flow at the sail/hull junction, but a full description of the complex interactions would require visualization in the flowfield, as well as on the surface of the model.

Where comparison has been possible, reasonable agreement was found with other observations. Hull separation appeared to start further forward than Spangler's data for missile noses[12] suggests. The results for junction flow generally supported the interpretation of Dickinson[10].

The results presented here will prove useful in interpreting other tests with the systematic series represented by these models.

ACKNOWLEDGEMENTS

The help of Keith Hansen, and the operators of the NAE 2 x 3 m wind tunnel, in performing these experiments, is gratefully acknowledged. Thanks are also due to Dick Wickens for some valuable discussions on the interpretation of results from this technique; however, the interpretations presented here are the author's own.

TABLE I . SUMMARY OF TEST PARAMETERS

Test	Nose	Sail	R_e million	Pitch deg.	Yaw deg.
1	Axisymmetric	None	7.0	4,8,12,16,20	0
2	Axisymmetric	None	4.9,9.5	12	0
3	Axisymmetric	F	7.0	-12,12	0
4	Axisymmetric	F	7.0	0	0,8,12,16
5	Axisymmetric	S	7.0	0	8,12,16
6	Axisymmetric	S	4.9	0	16
7	Asymmetric	None	7.0	12,16	0
8	Asymmetric	None	7.0	0	8,12,16,20
9	Asymmetric	None	7.0	8.55	8.55
10	Asymmetric	S	7.0	-12,12	0
11	Asymmetric	S	7.0	0	8,12,16,20
12	Asymmetric	S	7.0	-8.55,8.55	8.55

Notes:

- For tests 1 and 2, axisymmetry means that pitch and yaw are equivalent. In the text, the angular variations for these tests are therefore referred to as incidence.

- In tests 9 and 12, the model was first rotated 45 degrees about the longitudinal axis of the hull; then the turntable was rotated 12 degrees for test 9 and ±12 degrees for test 12.

(a) GENERAL ARRANGEMENT

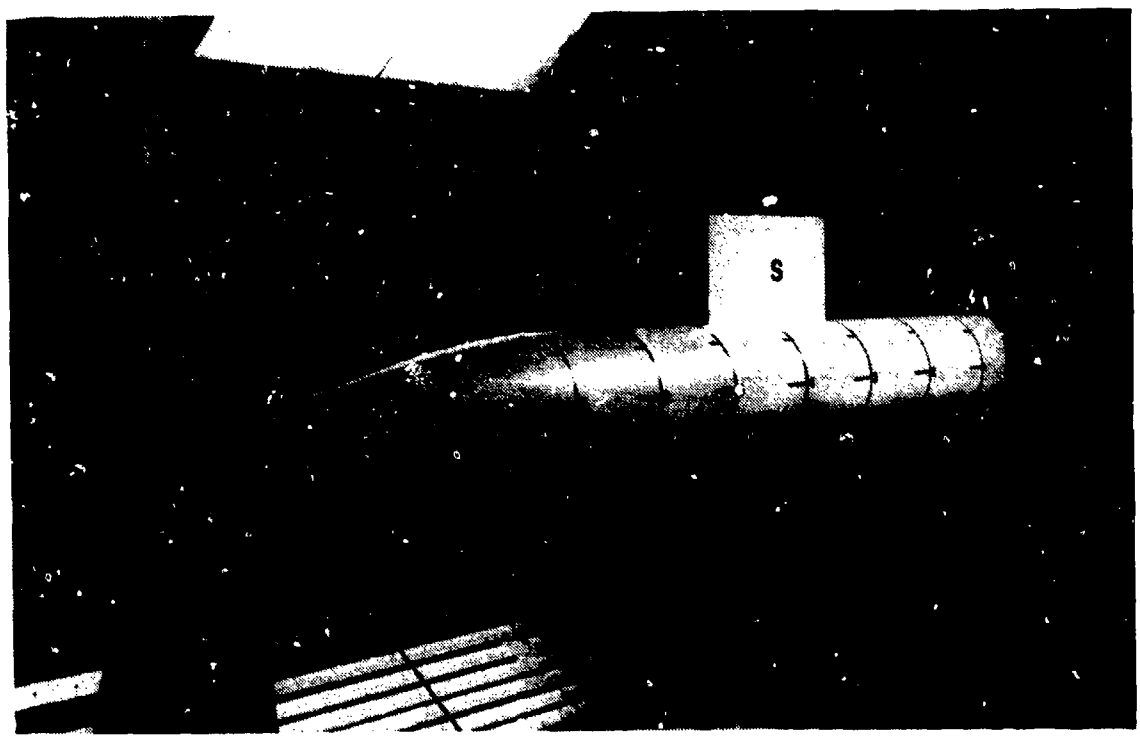

(b) ASYMMETRIC HULL WITH SAIL S

FIG. 1 WINDTUNNEL AND MODEL

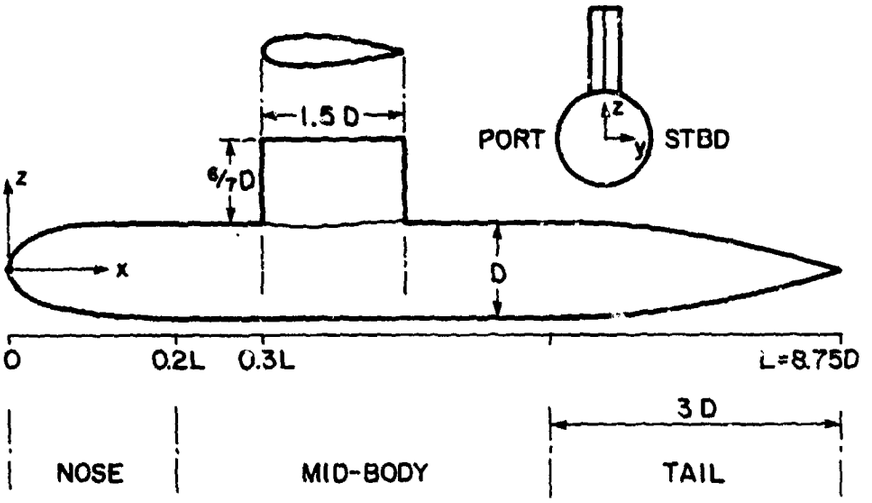

FIG. 2 SUBMARINE MODEL, PRINCPAL DIMENSIONS

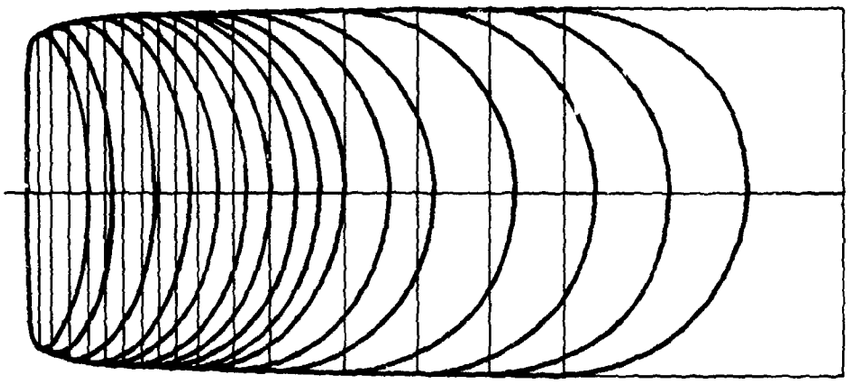

FIG. 3 ASYMMETRIC NOSE, SHOWING CROSS-SECTIONS

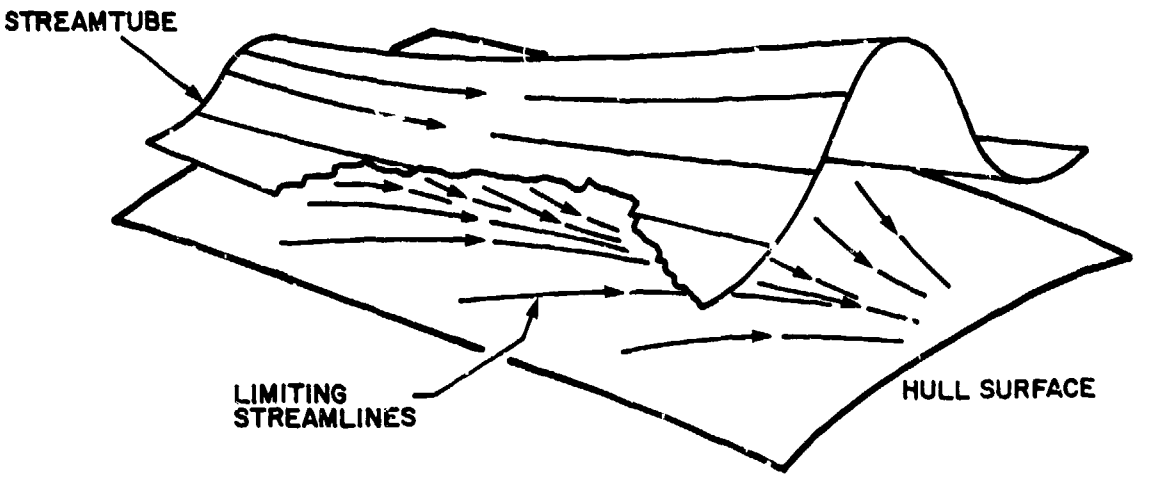

(a) THREE DIMENSIONAL SEPARATION OF FREE SHEAR LAYER

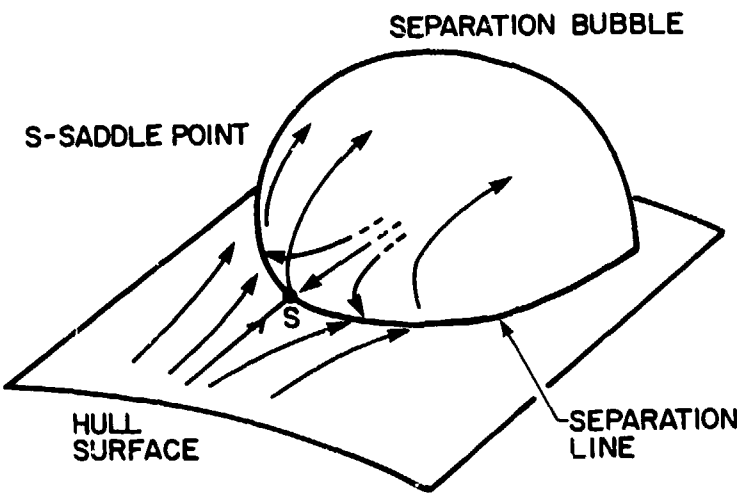

(b) THREE DIMENSIONAL BUBBLE SEPARATION

FIG. 4 MECHANISMS FOR SEPARATION

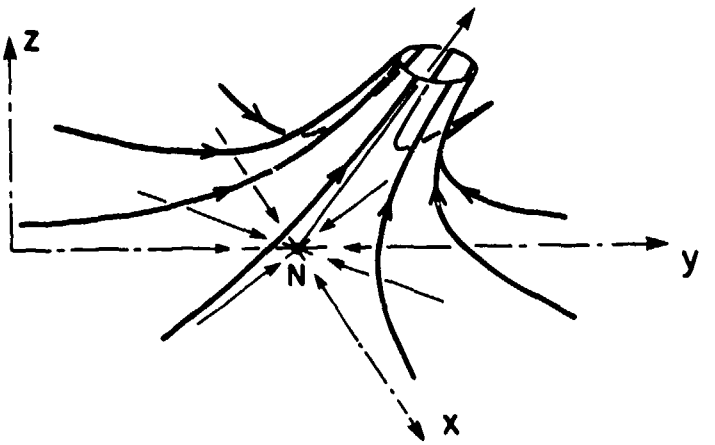

(a) NODE (OF SEPARATION)

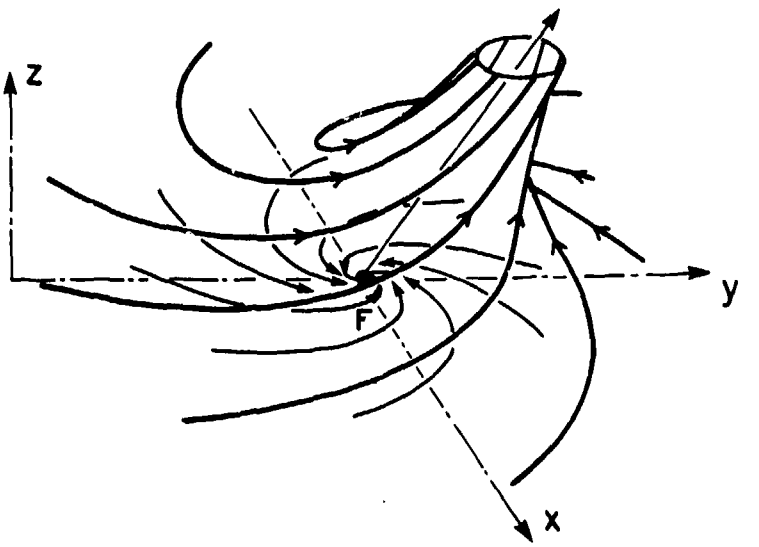

(b) FOCUS (OF SEPARATION)

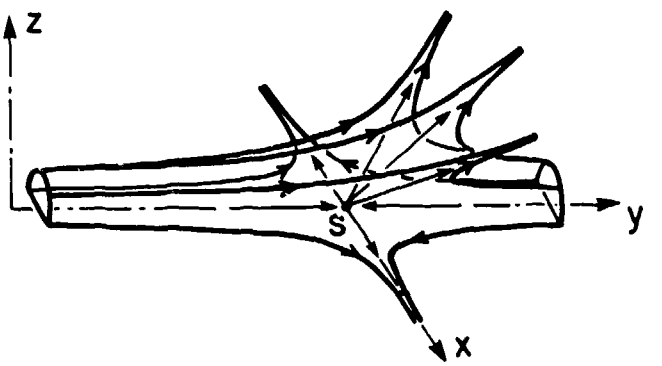

(c) SADDLE POINT

FIG. 5 SINGULAR POINTS (FROM REFERENCE 6)

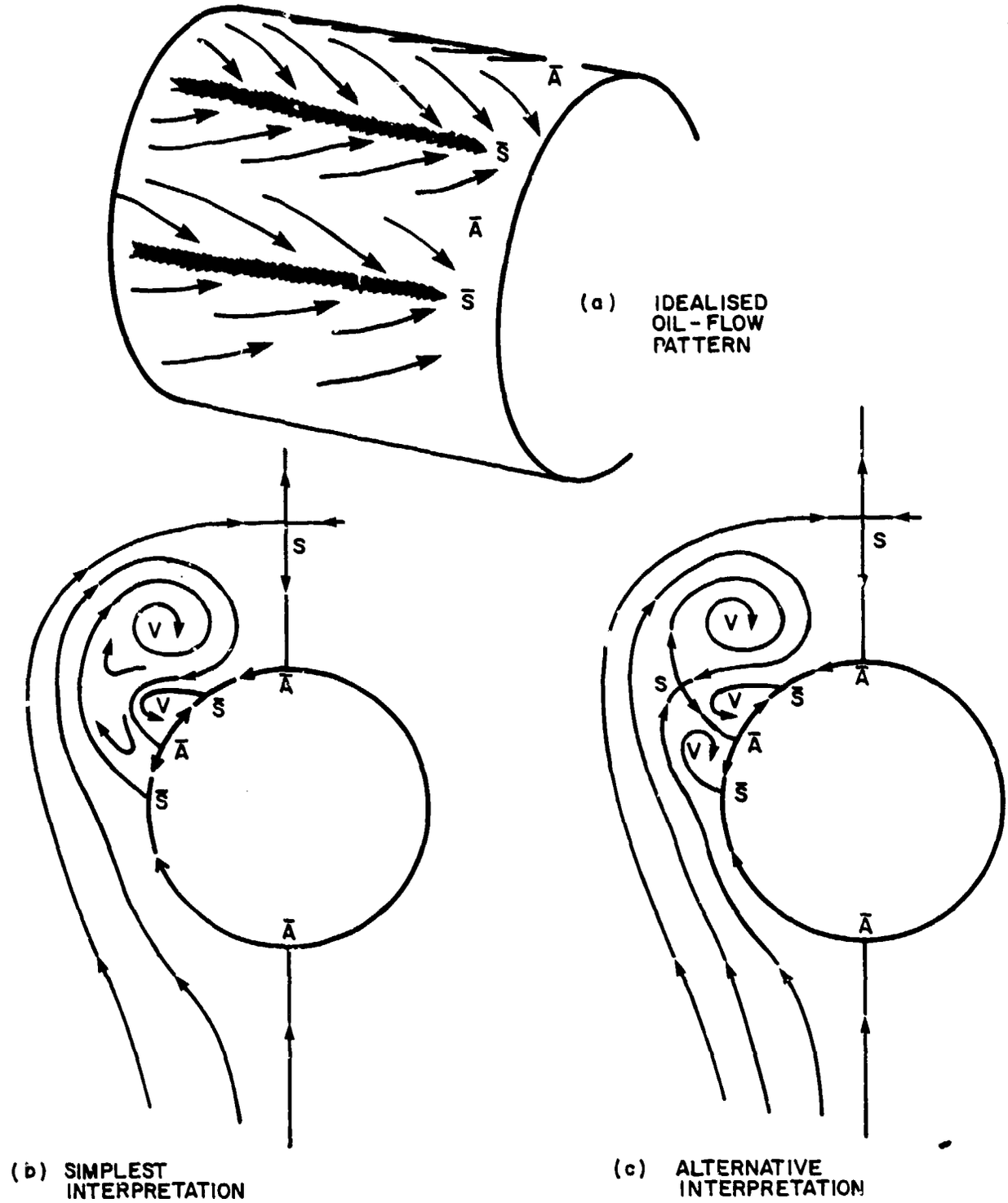

FIG 6 SHEAR STRESS ON A CIRCULAR CYLINDER AT INCIDENCE

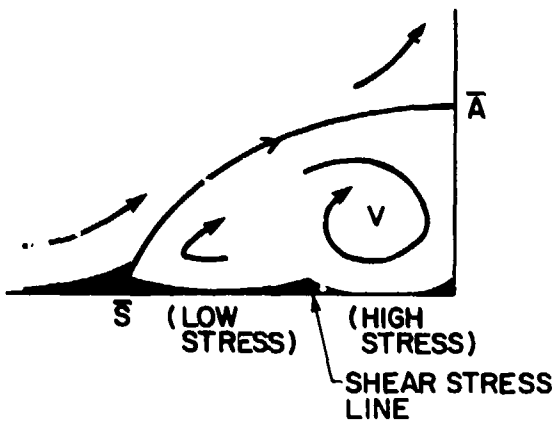

(a) FORMATION OF A SHEAR STRESS LINE

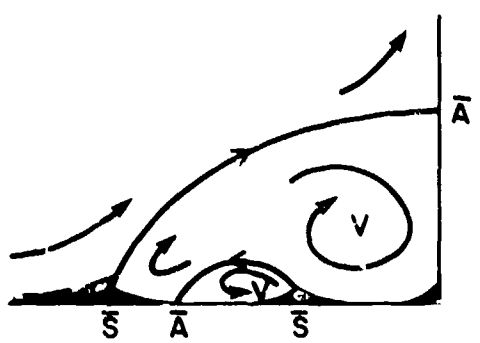

(b) FORMATION OF SECONDARY VORTEX

FIG. 7 POSSIBLE EVOLUTION OF A CORNER FLOW

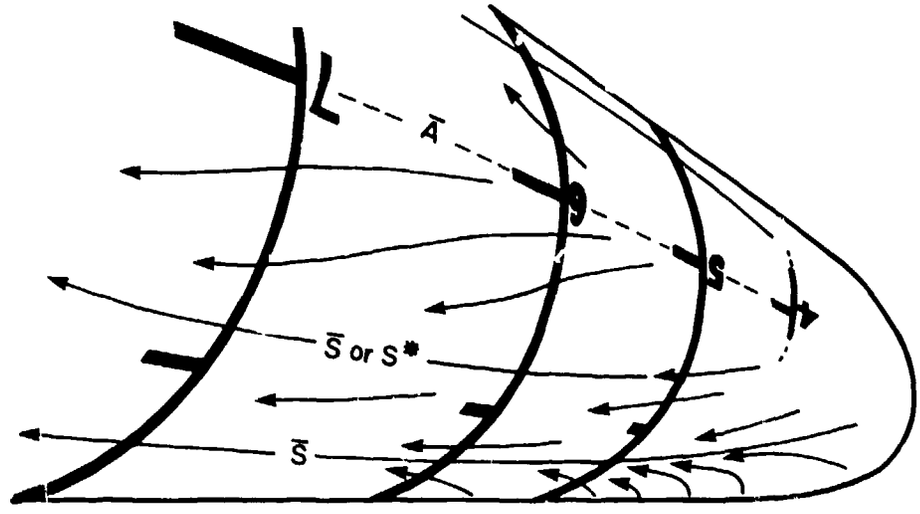

FIG. 8 AXISYMMETRIC HULL AT 12° INCIDENCE : LEEWARD VIEW

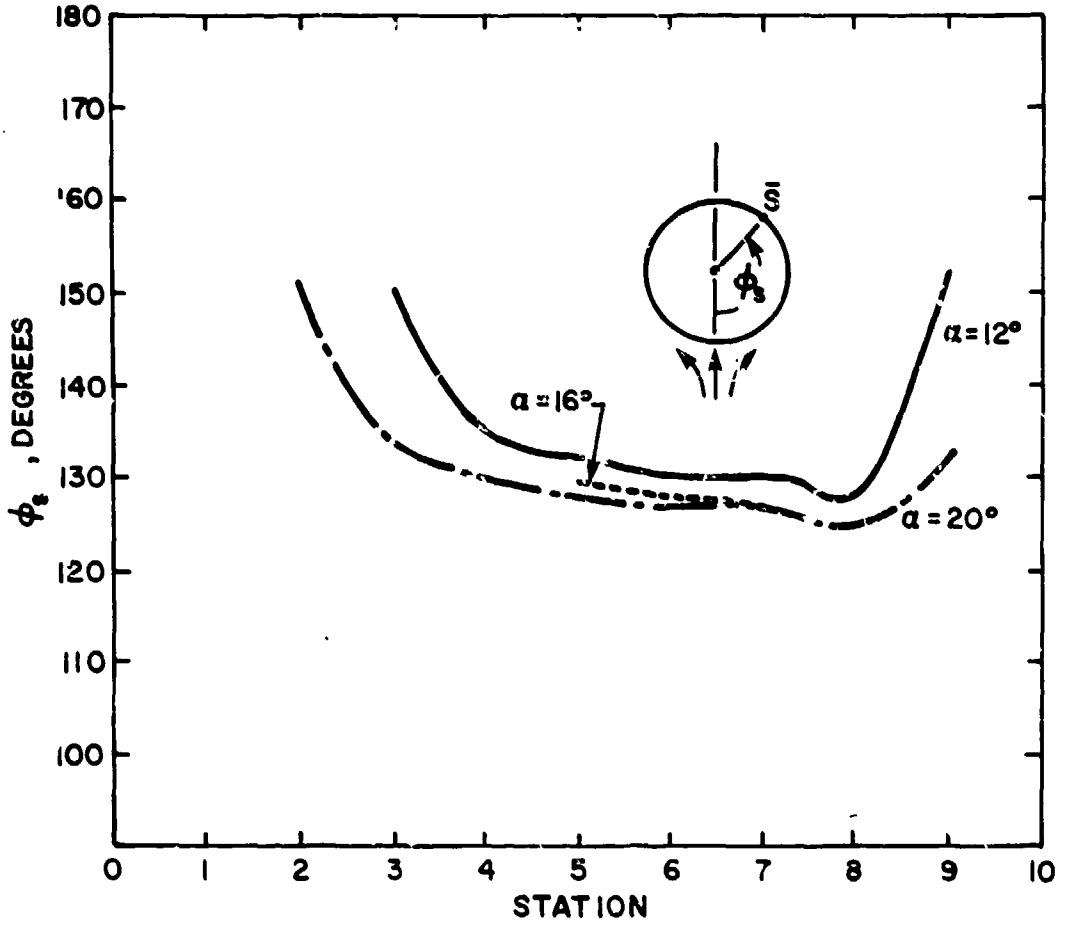

FIG. 9 LOCATION OF PRIMARY SEPARATION LINE FOR AXISYMMETRIC HULL ALONE

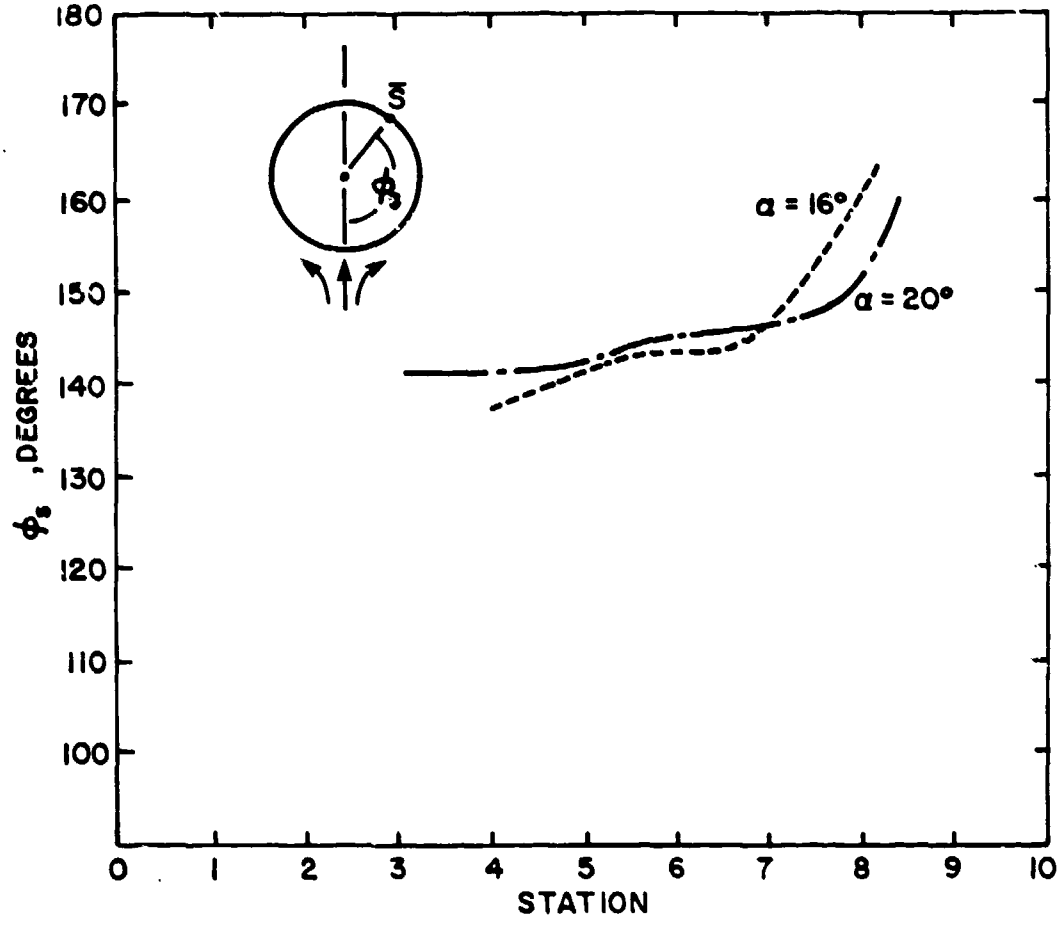

FIG. 10 LOCATION OF SECONDARY SEPARATION LINE FOR AXISYMMETRIC HULL ALONE

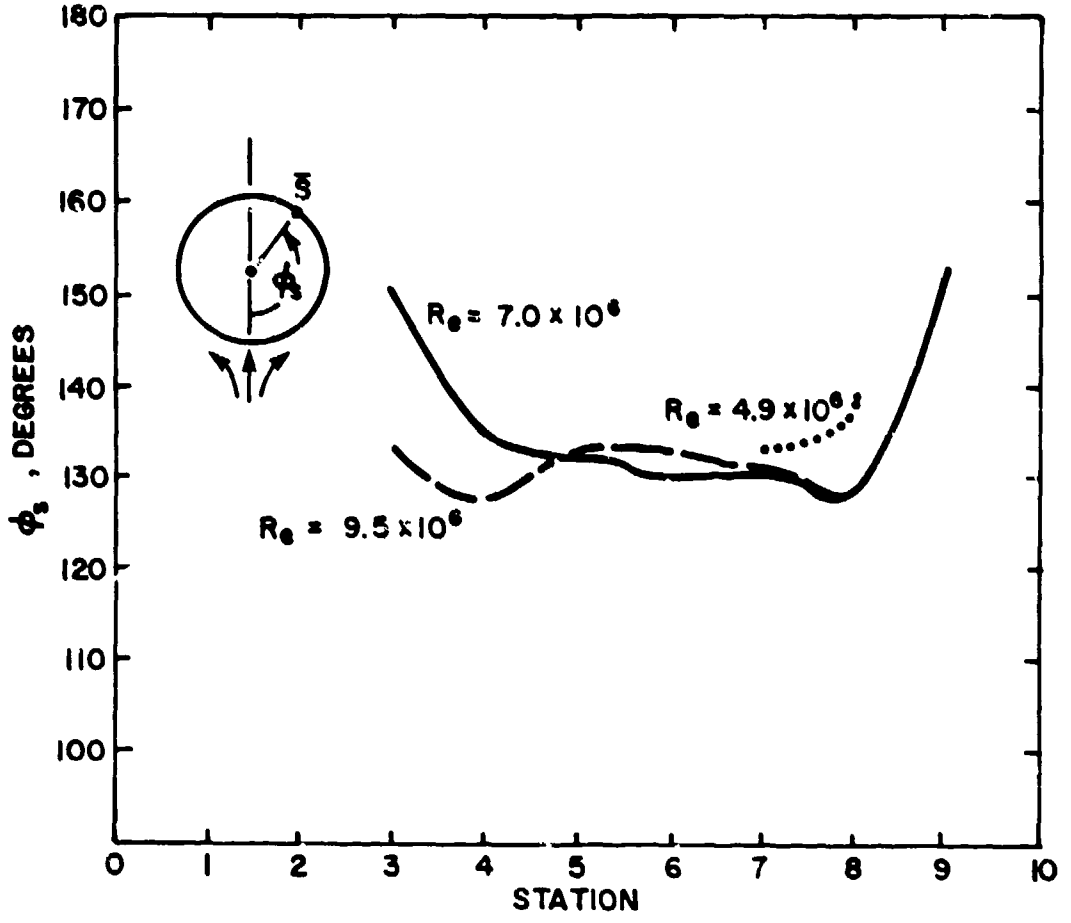

FIG. 11 LOCATION OF PRIMARY SEPARATION LINE FOR AXISYMMETRIC HULL ALONE AT 12° INCIDENCE : REYNOLDS NUMBER VARIATIONS

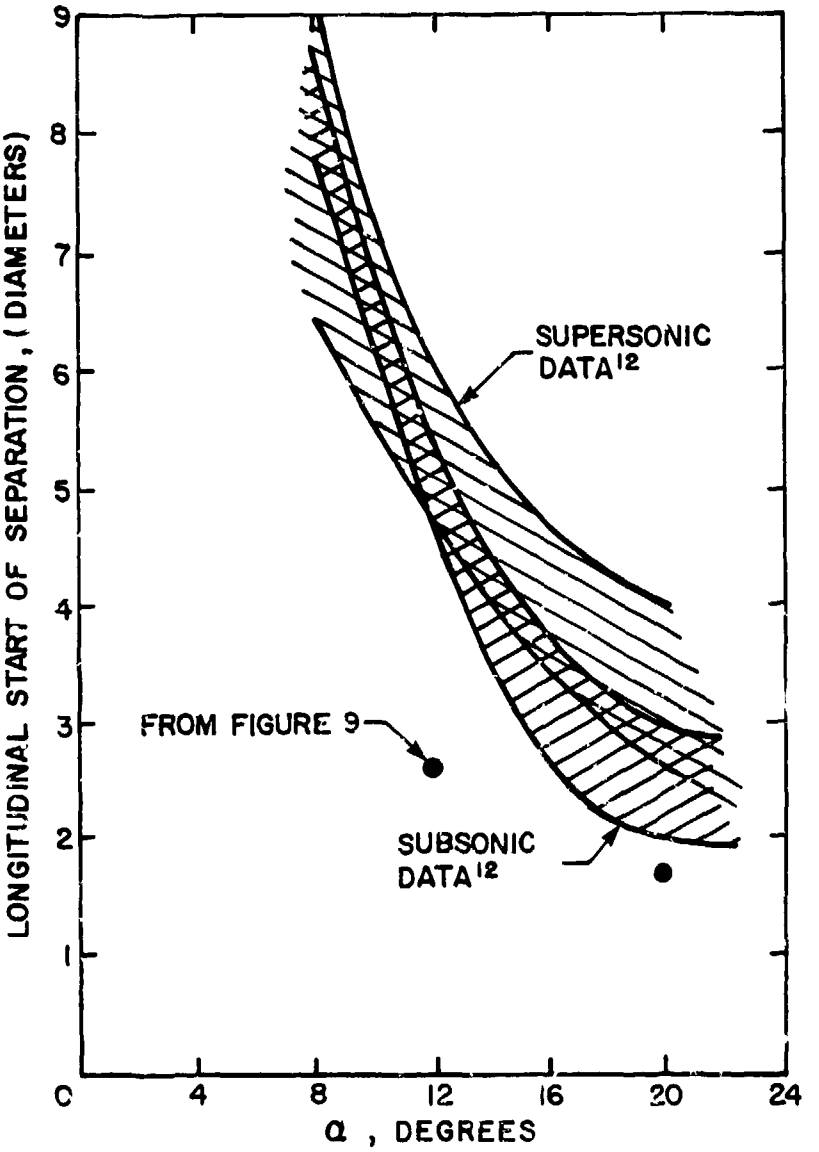

FIG. 12 LONGITUDINAL START OF SEPARATION FOR BODIES OF REVOLUTION (FROM REFERENCE 12)

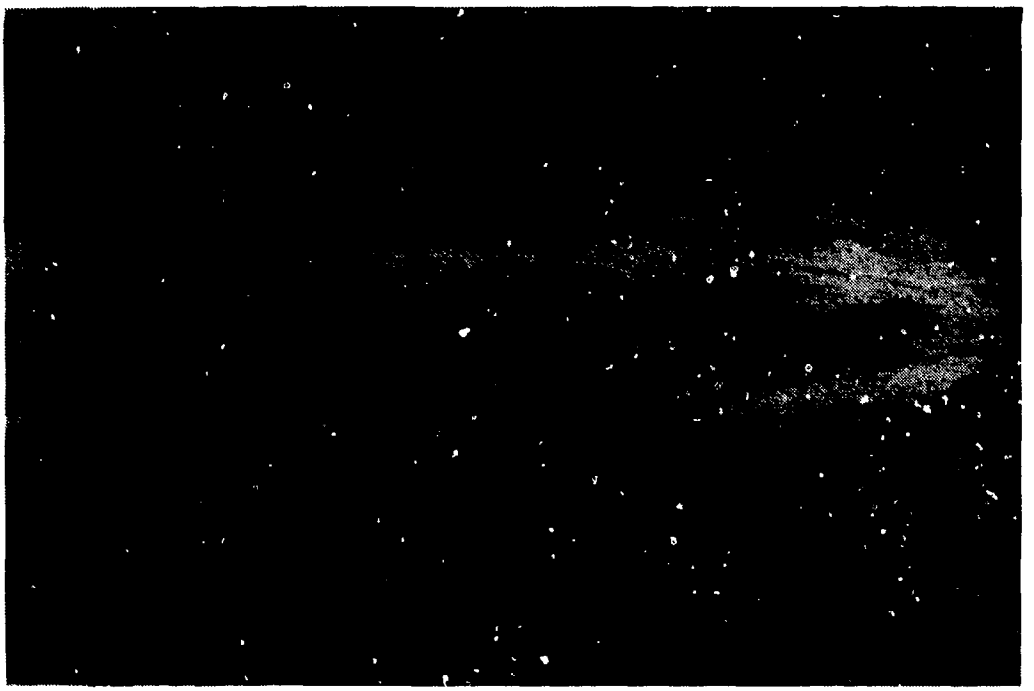

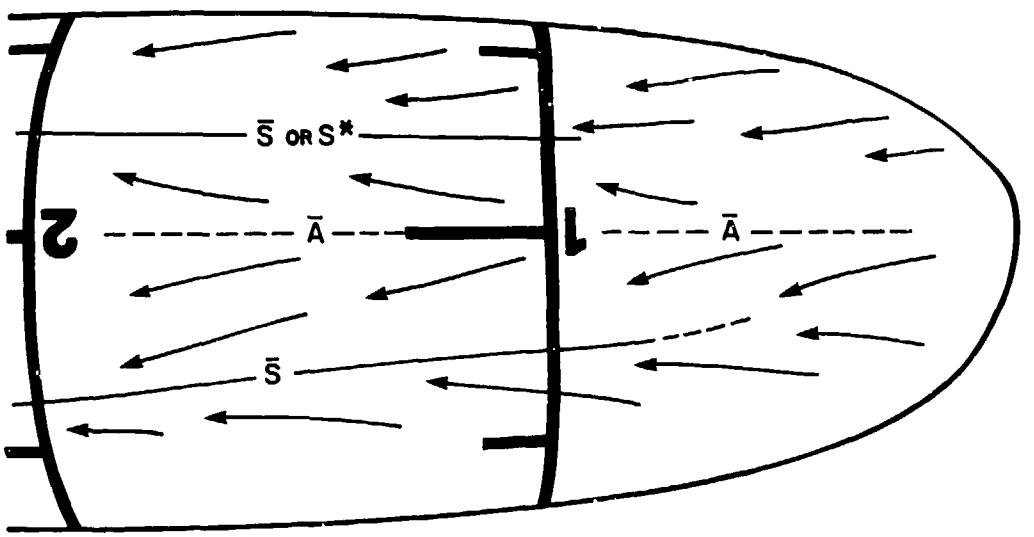

FIG. 13 ASYMMETRIC HULL AT 12° PITCH : LEEWARD VIEW

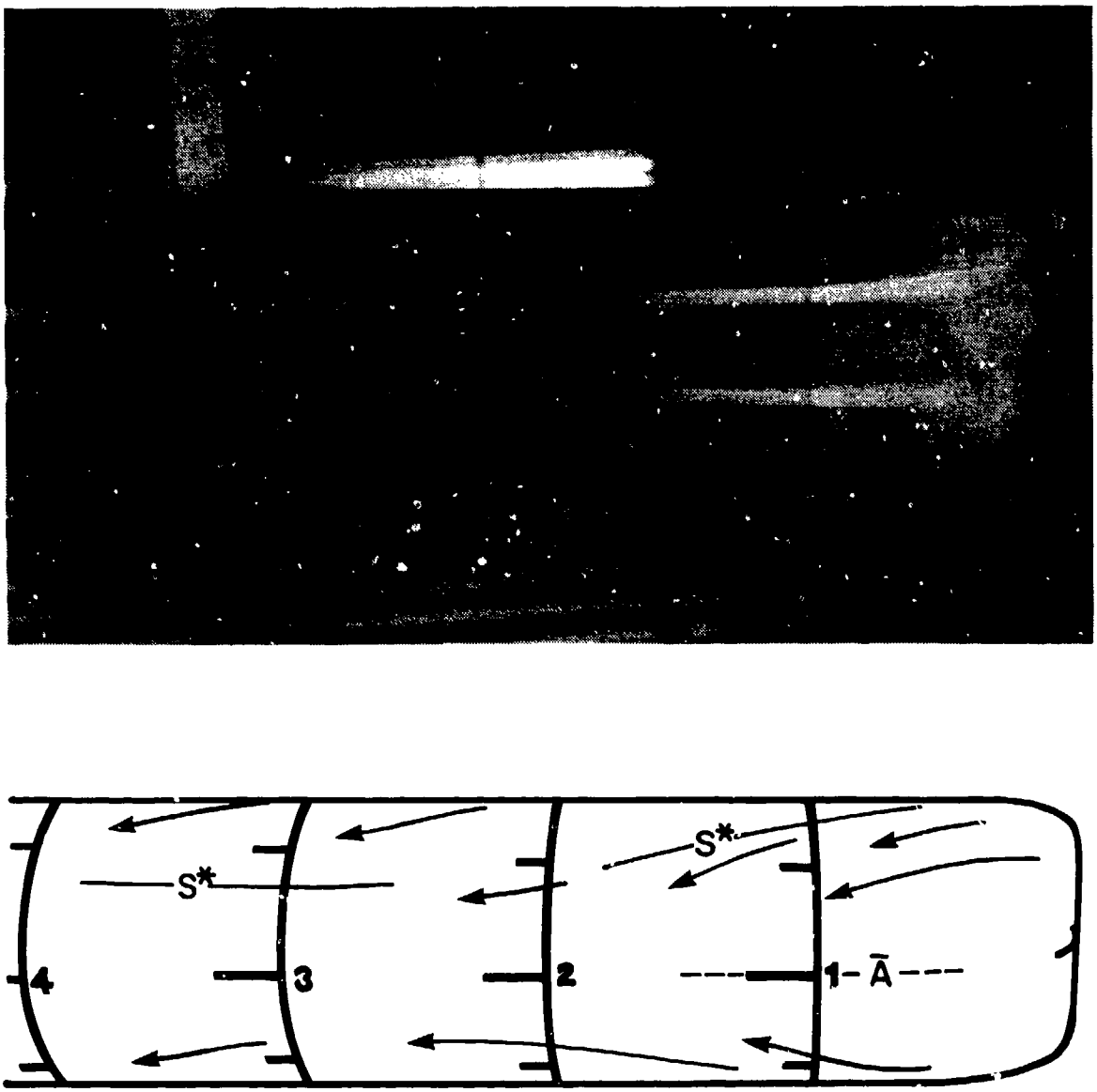

FIG. 14 ASYMMETRIC HULL AT 12° YAW : LEEWARD VIEW

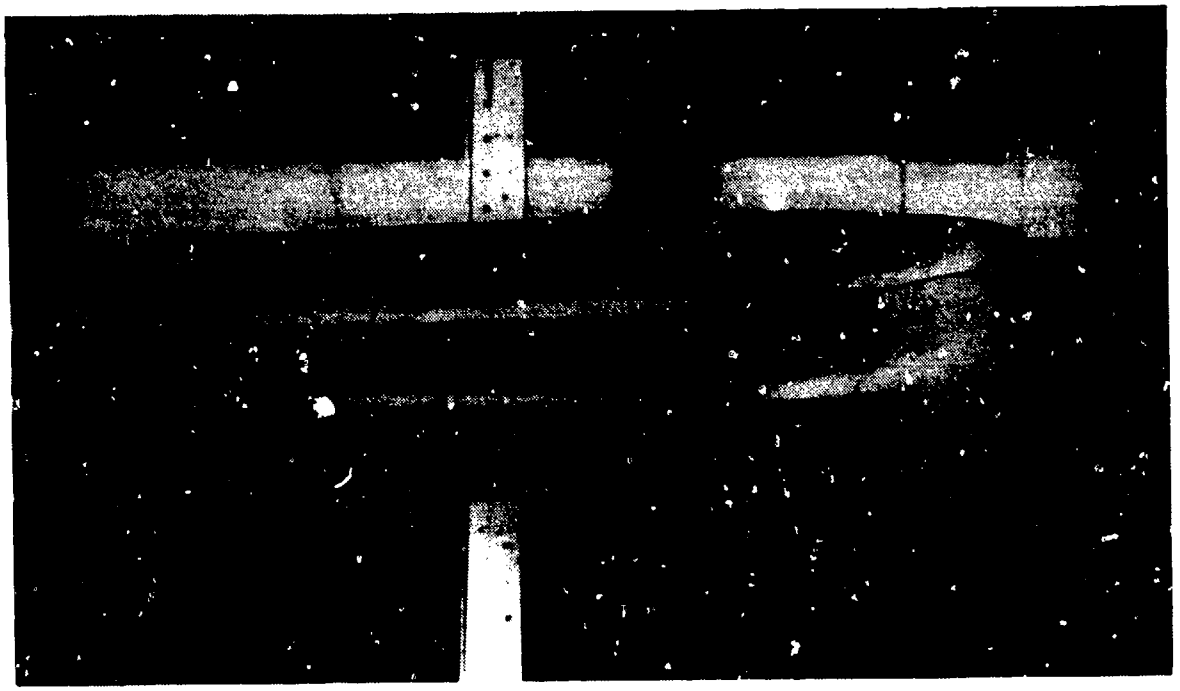

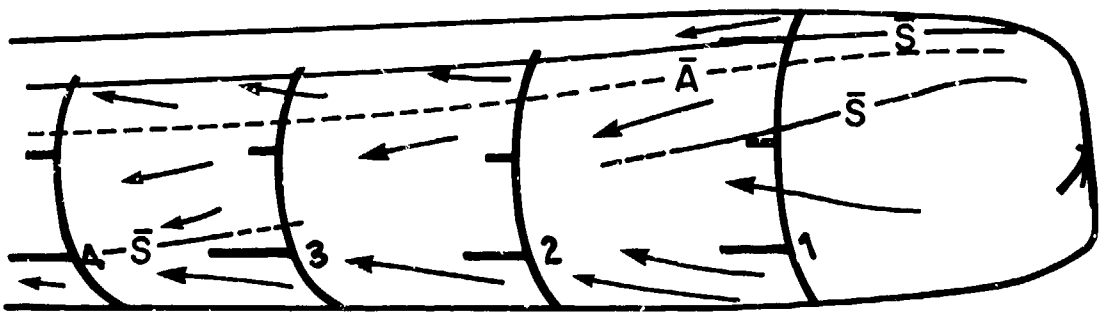

FIG. 15 ASYMMETRIC HULL AT 8.55° PITCH, 8.55° YAW : LEEWARD VIEW

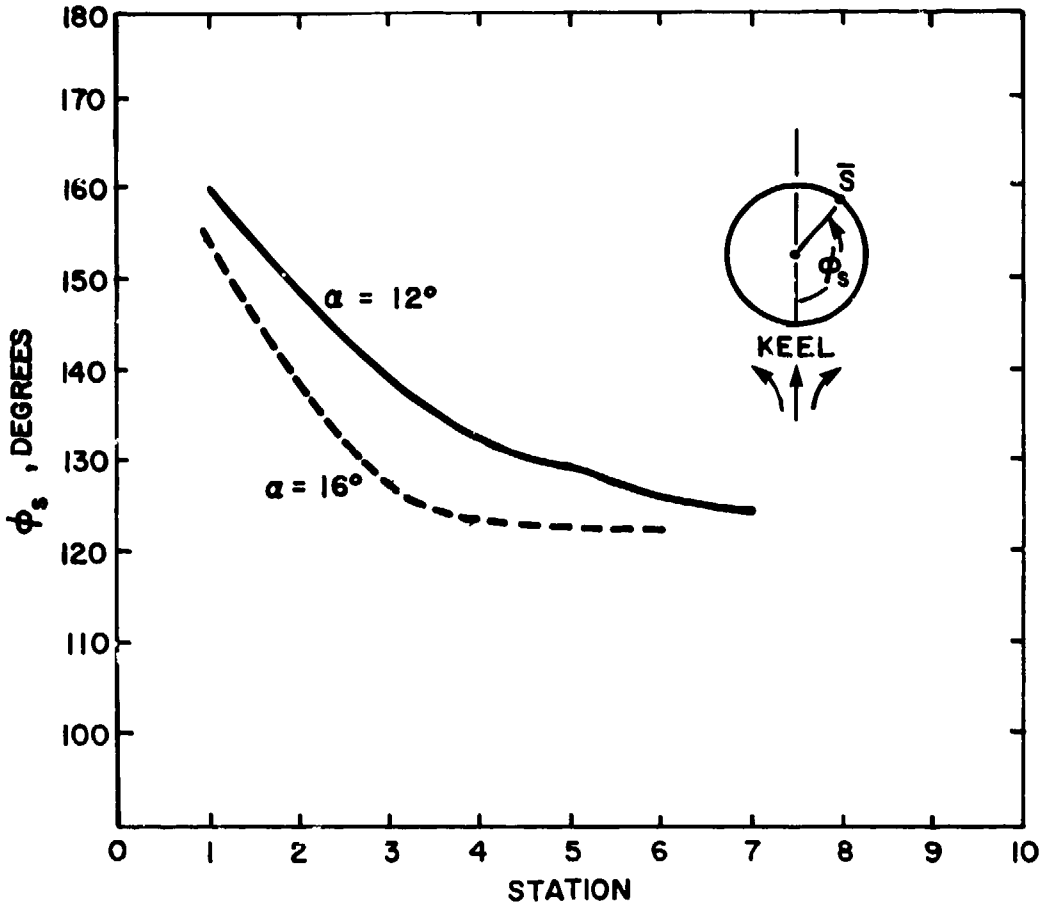

FIG. 16 LOCATION OF PRIMARY SEPARATION LINE FOR ASYMMETRIC HULL IN PITCH

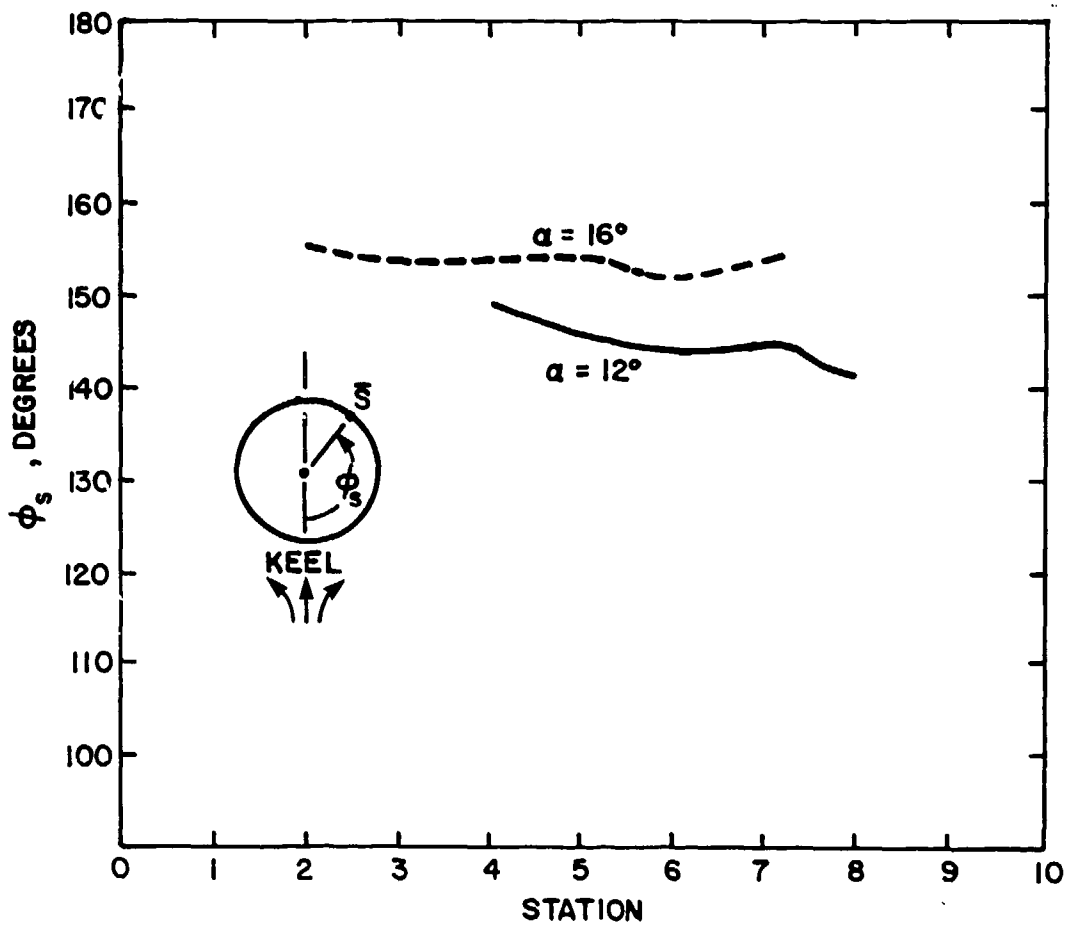

FIG. 17 LOCATION OF SECONDARY SEPARATION LINE FOR ASYMMETRIC HULL IN PITCH

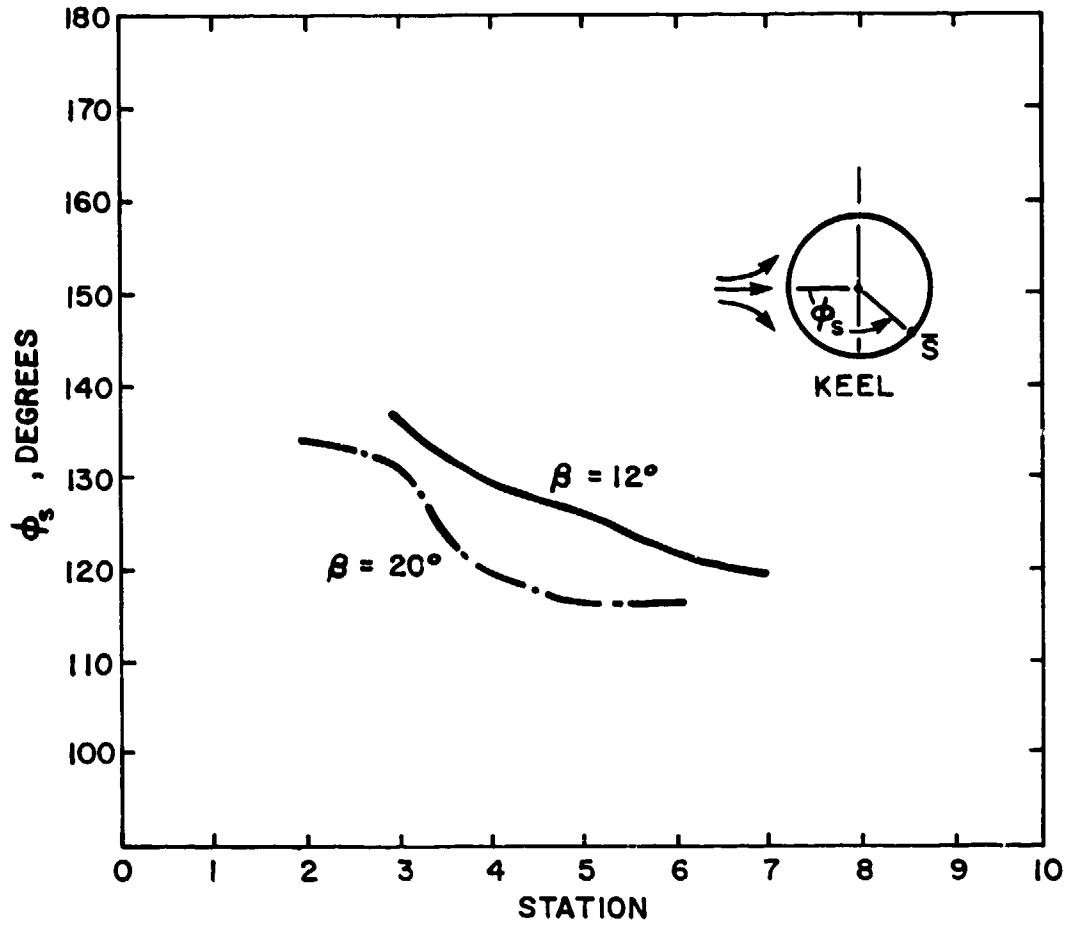

FIG. 18 LOCATION OF PRIMARY SEPARATION LINE FOR ASYMMETRIC HULL IN YAW

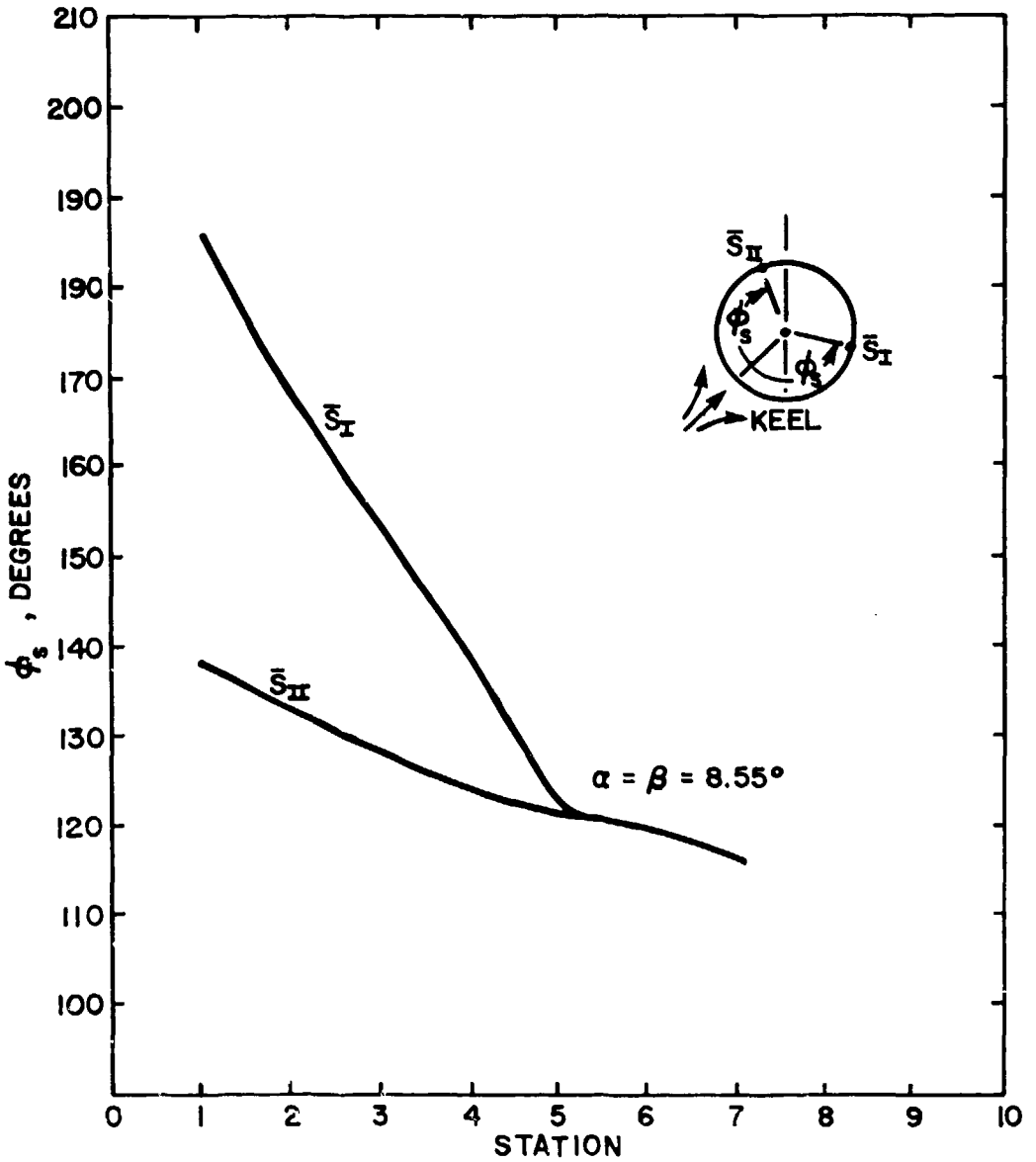

FIG. 19 LOCATION OF PRIMARY SEPARATION LINES FOR ASYMMETRIC HULL IN PITCH AND YAW

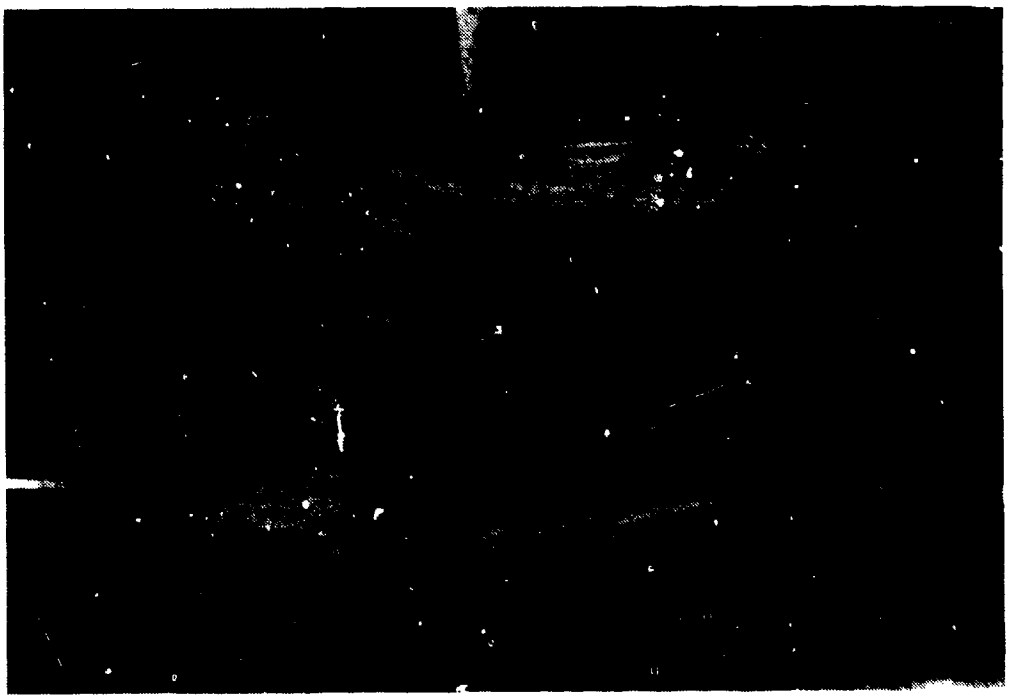

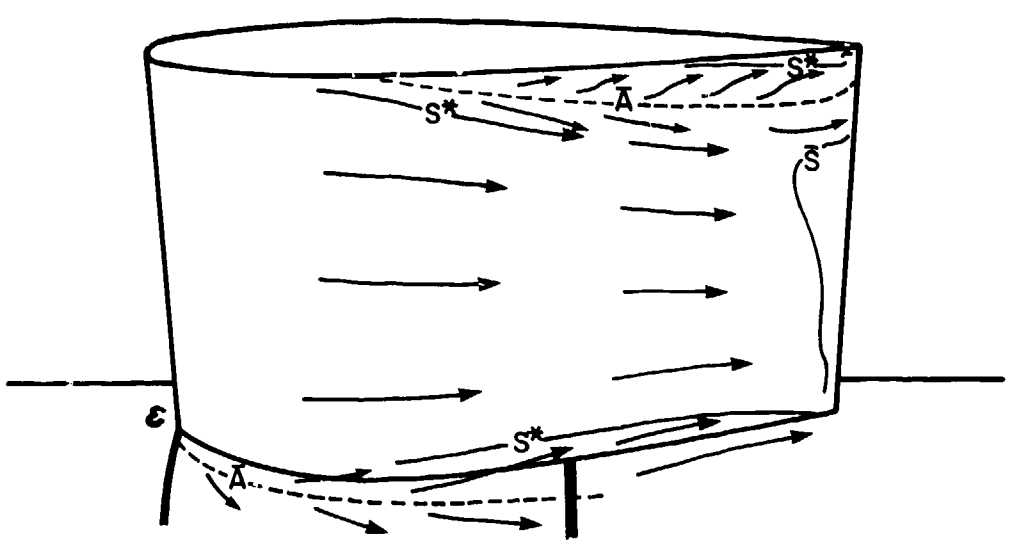

FIG. 20 SAIL F (ON AXISYMMETRIC HULL) IN AXIAL FLOW

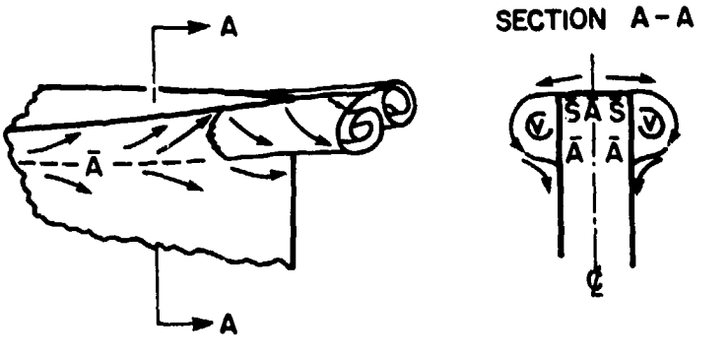

FIG. 21 SAIL TIP TRAILING EDGE VORTICES

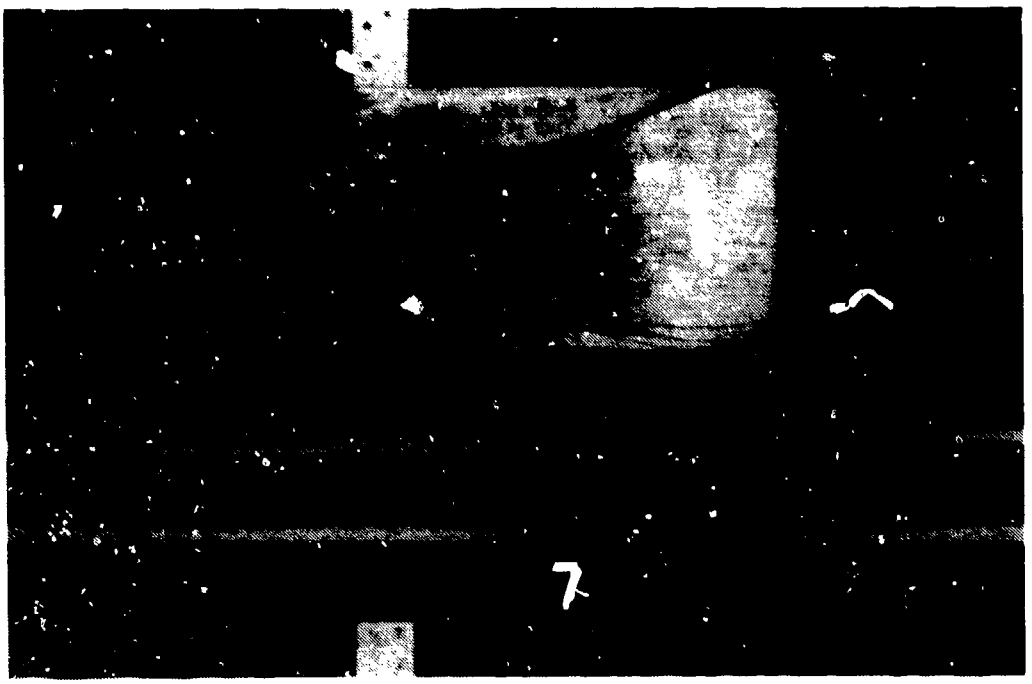

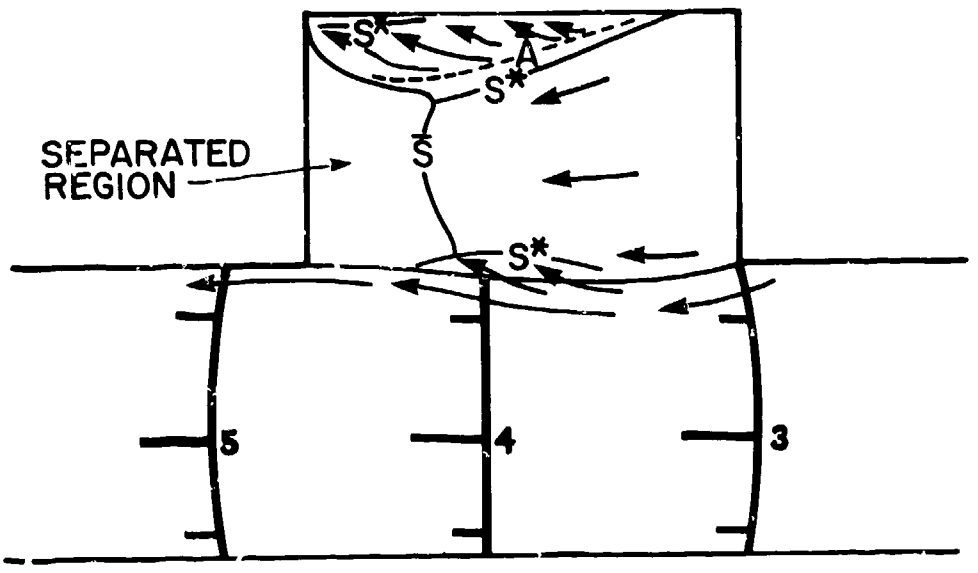

FIG. 22 SAIL F (ON AXISYMMETRIC HULL) AT 8° YAW : LEEWARD SIDE

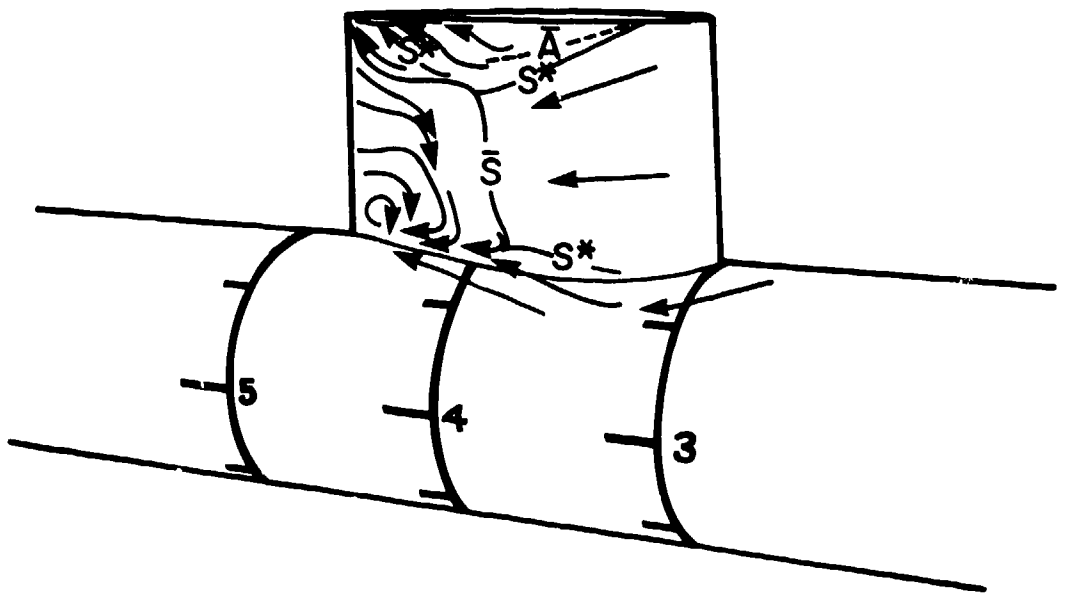

FIG. 23 SAIL F (ON AXISYMMETRIC HULL) AT 12° : LEEWARD SIDE

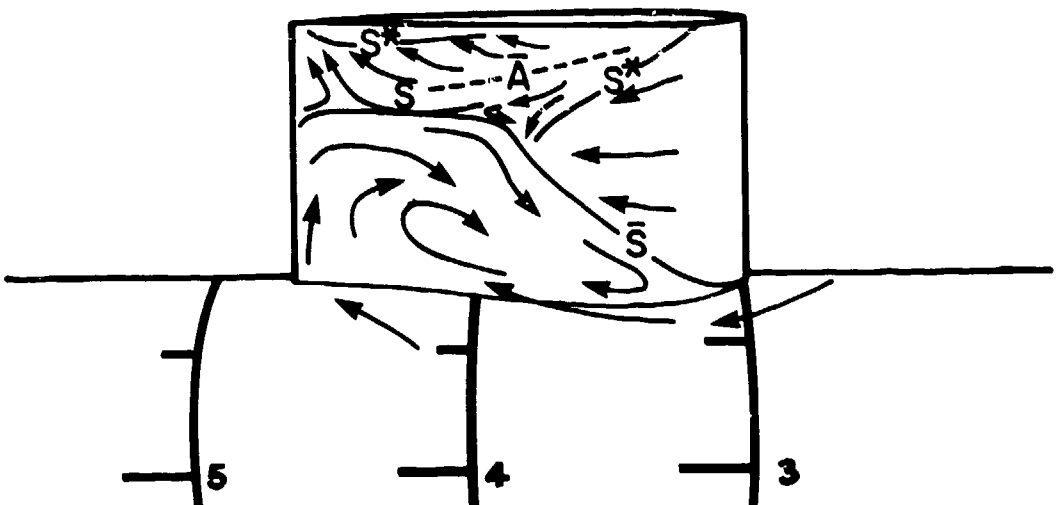

FIG. 24 SAIL F (ON AXISYMMETRIC HULL) AT 16° YAW : LEEWARD SIDE

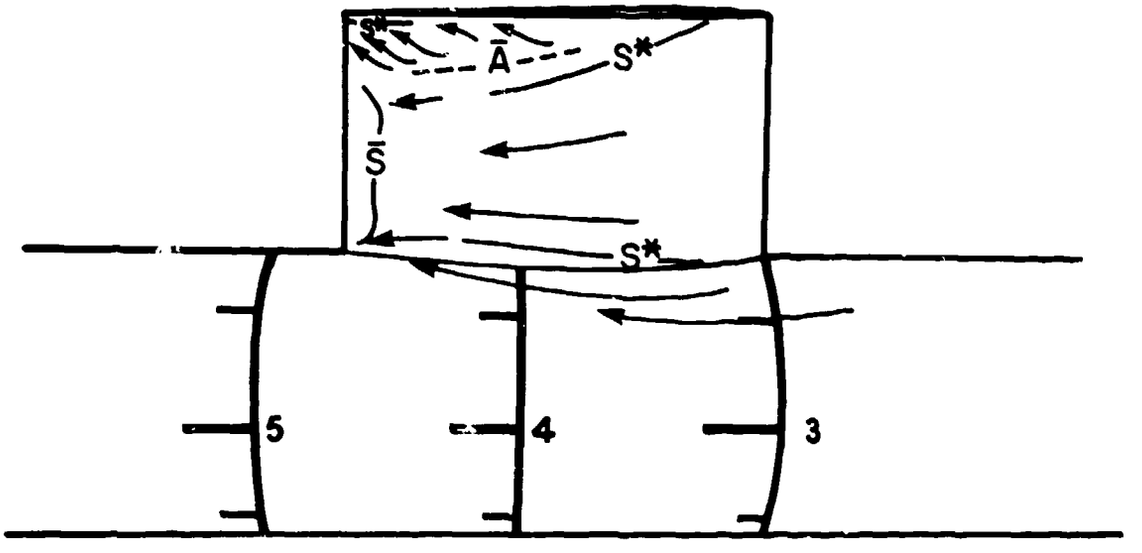

FIG. 25 SAIL S (ON AXISYMMETRIC HULL) AT 8° YAW : LEEWARD VIEW

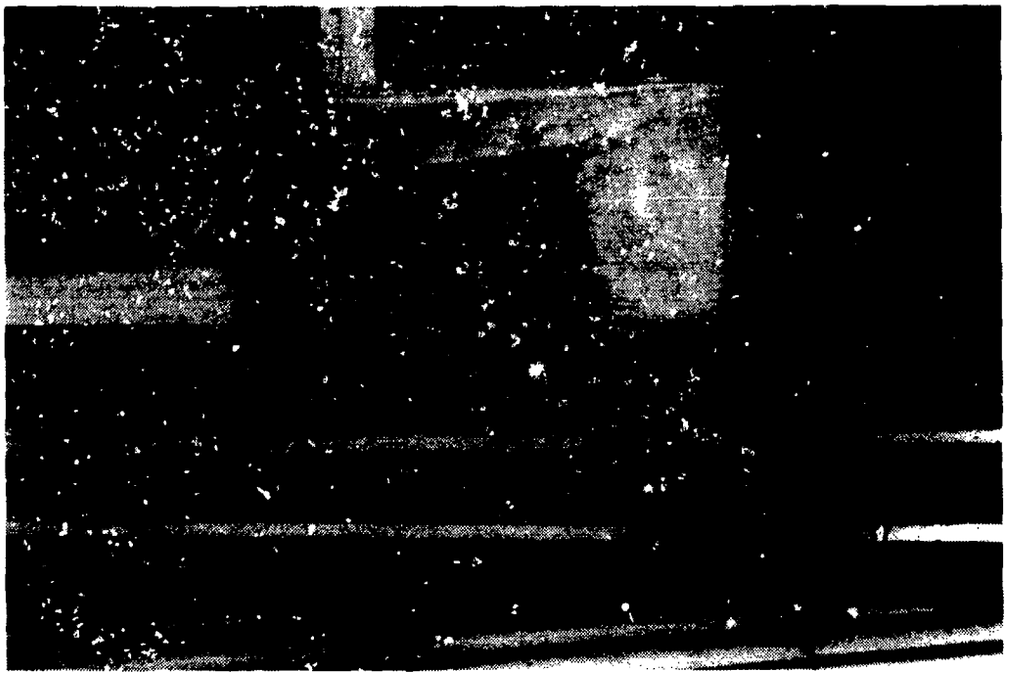

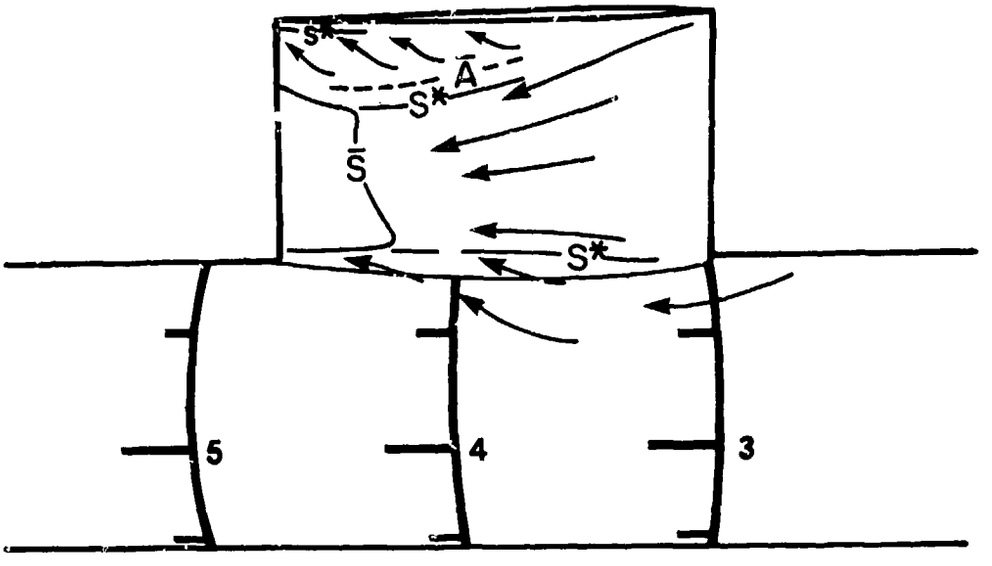

FIG. 26 SAIL S (ON AXISYMMETRIC HULL) AT 12° YAW : LEEWARD VIEW

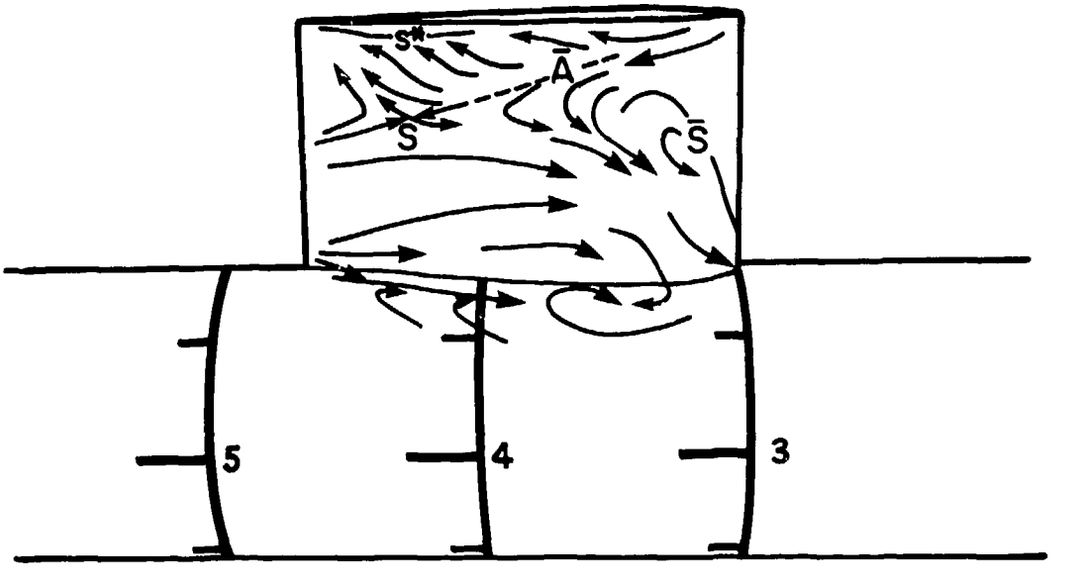

FIG. 27 SAIL S (ON AXISYMMETRIC HULL) AT 16° YAW : LEEWARD VIEW

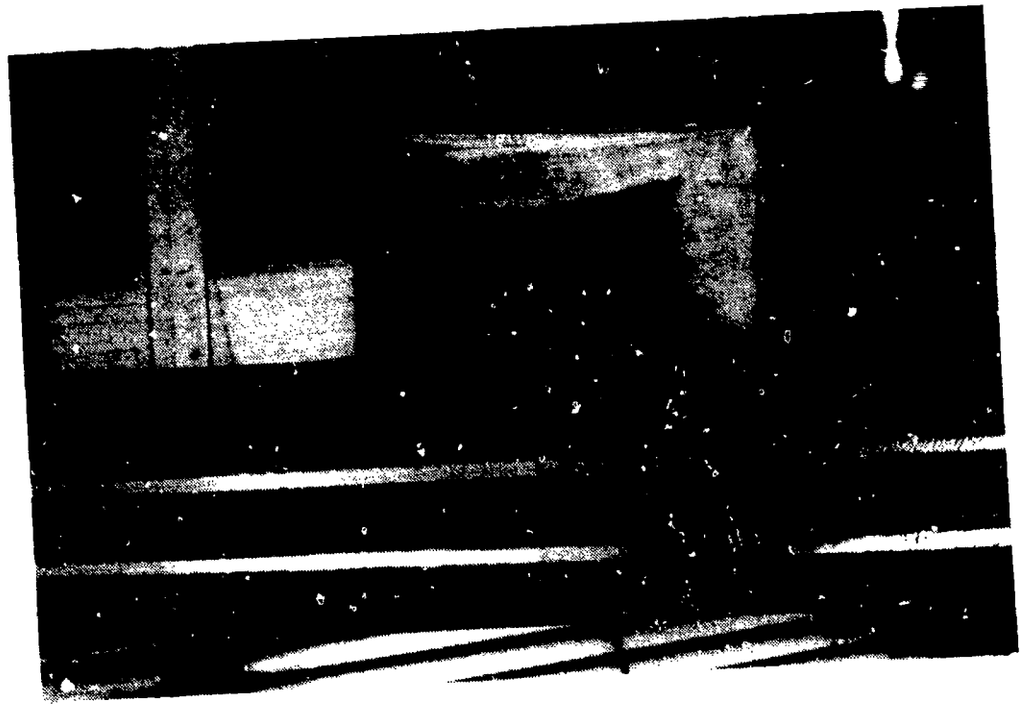

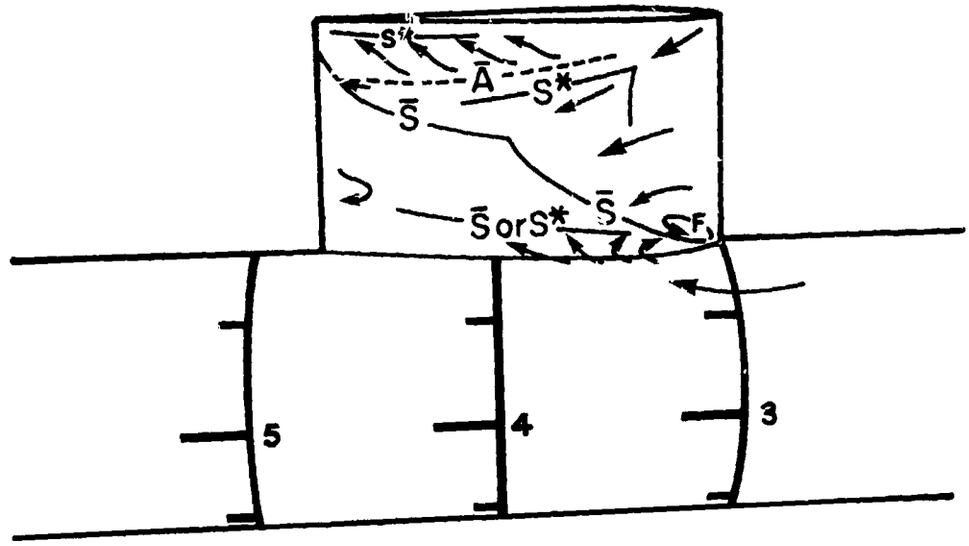

FIG. 28 SAIL S (ON AXISYMMETRIC HULL) AT 16° YAW : REYNOLDS NUMBER VARIATION, $R_e = 4.9 \times 10^6$

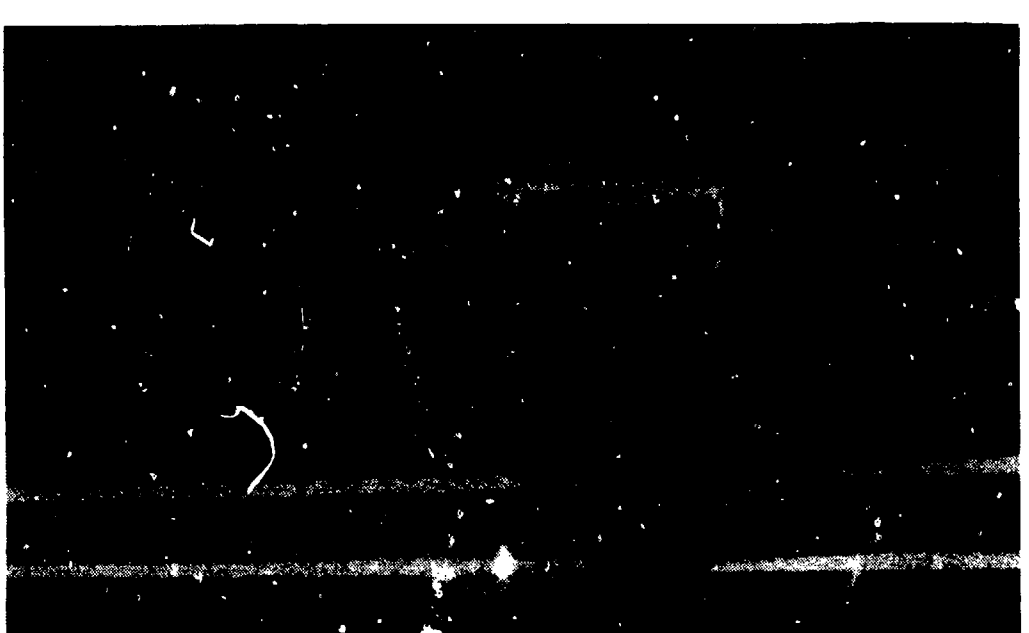

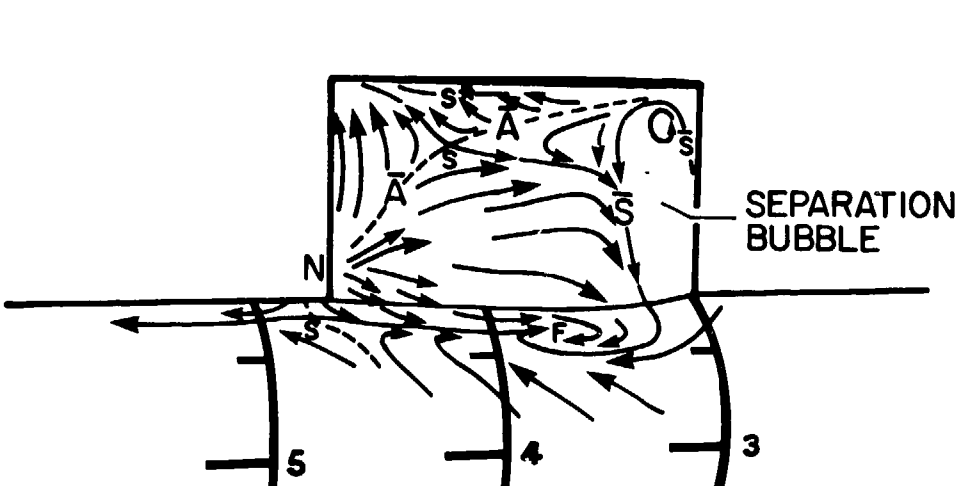

FIG. 29 SAIL S (ON ASYMMETRIC HULL) AT 20° YAW : LEEWARD SIDE

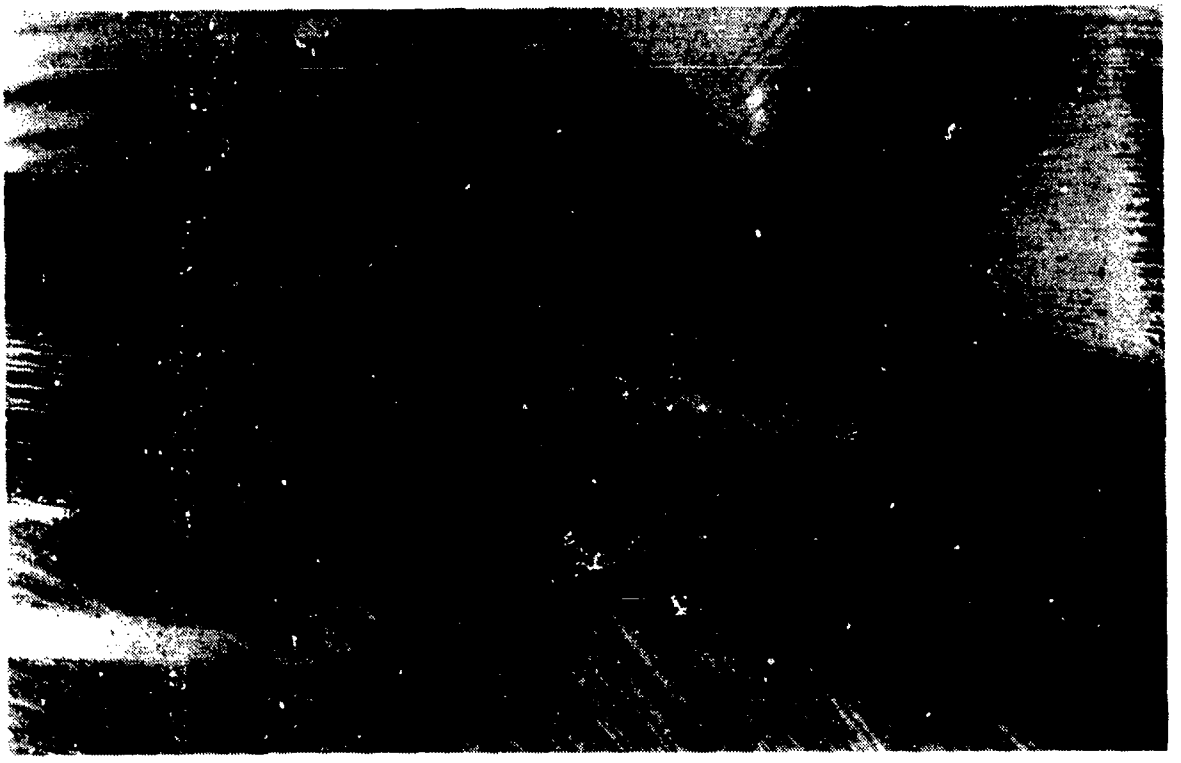

FIG. 30 SAIL S AT 20° YAW : SAIL TRAILING EDGE ROOT REGION

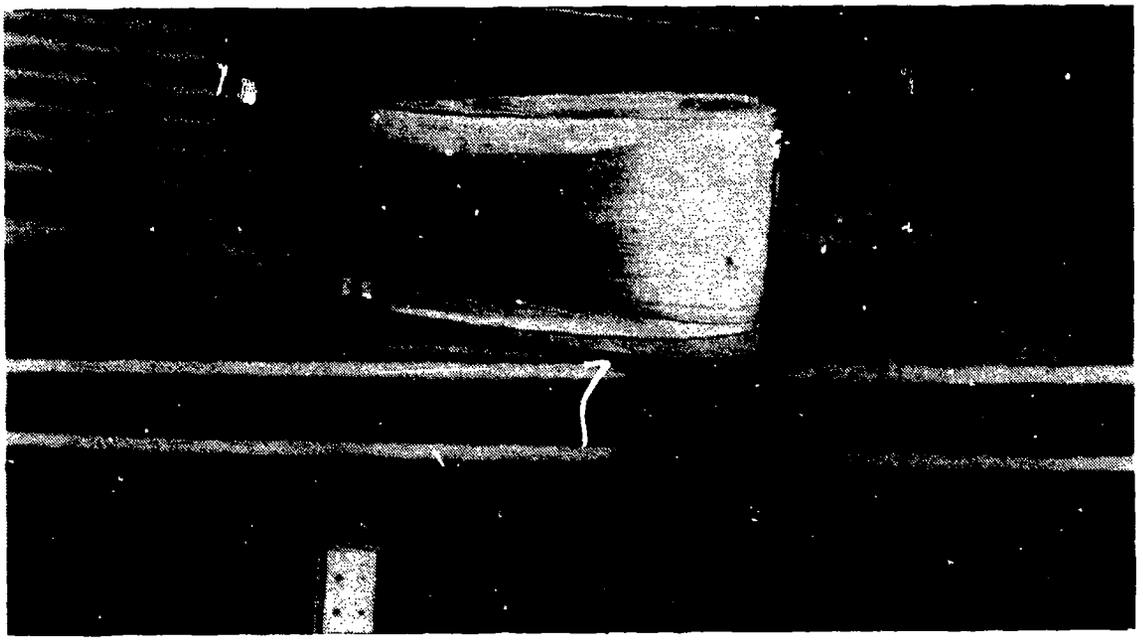

(a) α = 8.55°, β 8.55°

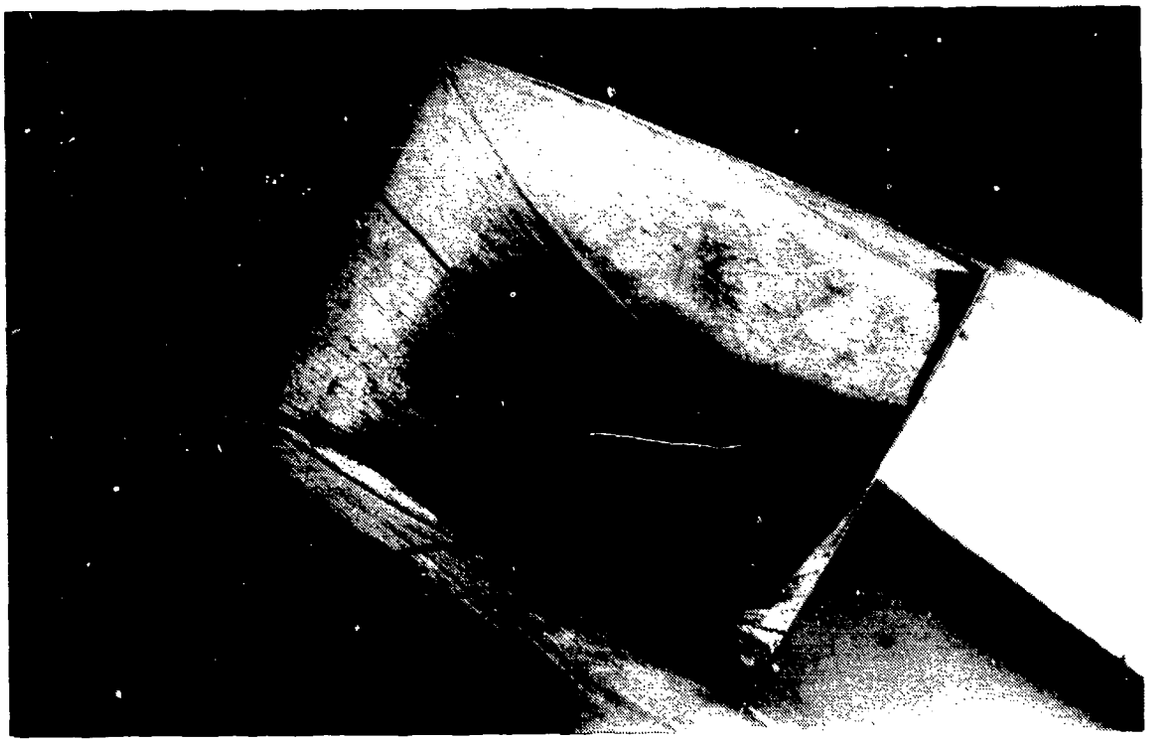

(b) α = -8.55°, β 8.55°

FIG. 31 SAIL S (ON ASYMMETRIC HULL) IN SIMULTANEOUS PITCH AND YAW

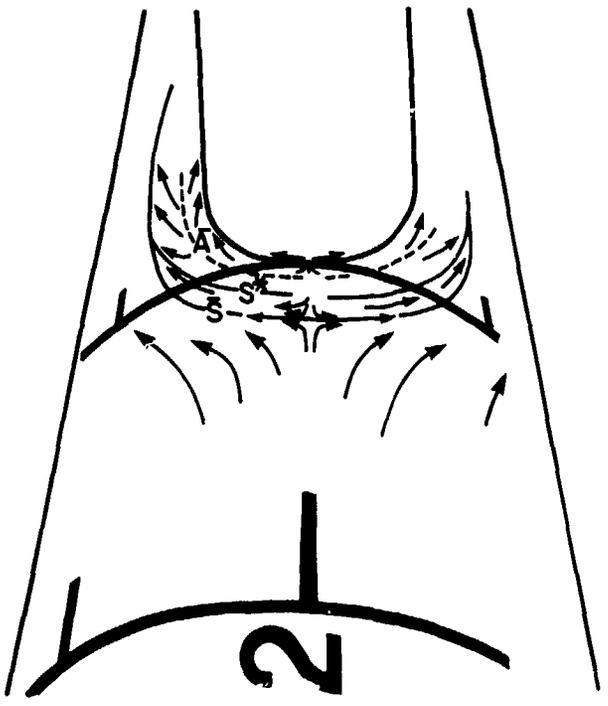

FIG. 32 SAIL F ON AXISYMMETRIC HULL IN AXIAL FLOW : DOWNSTREAM VIEW

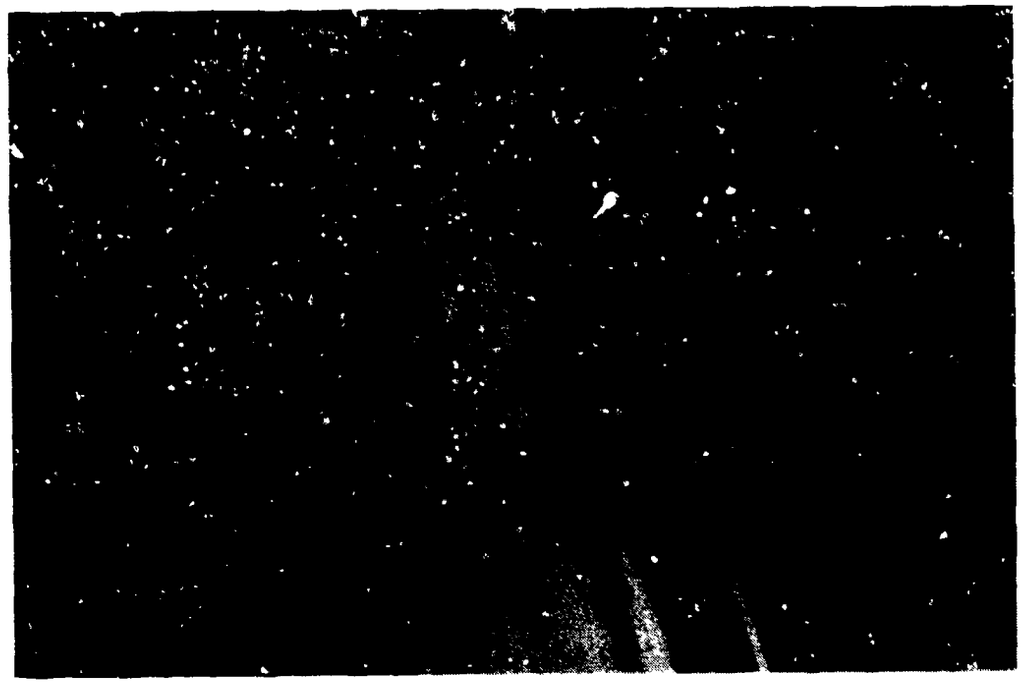

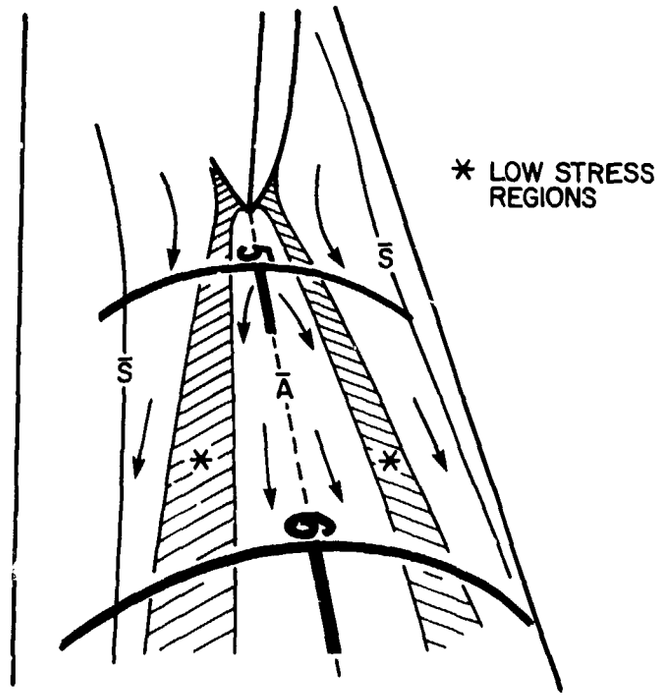

FIG. 33 SAIL F ON AXISYMMETRIC HULL IN A FLOW : UPSTREAM VIEW

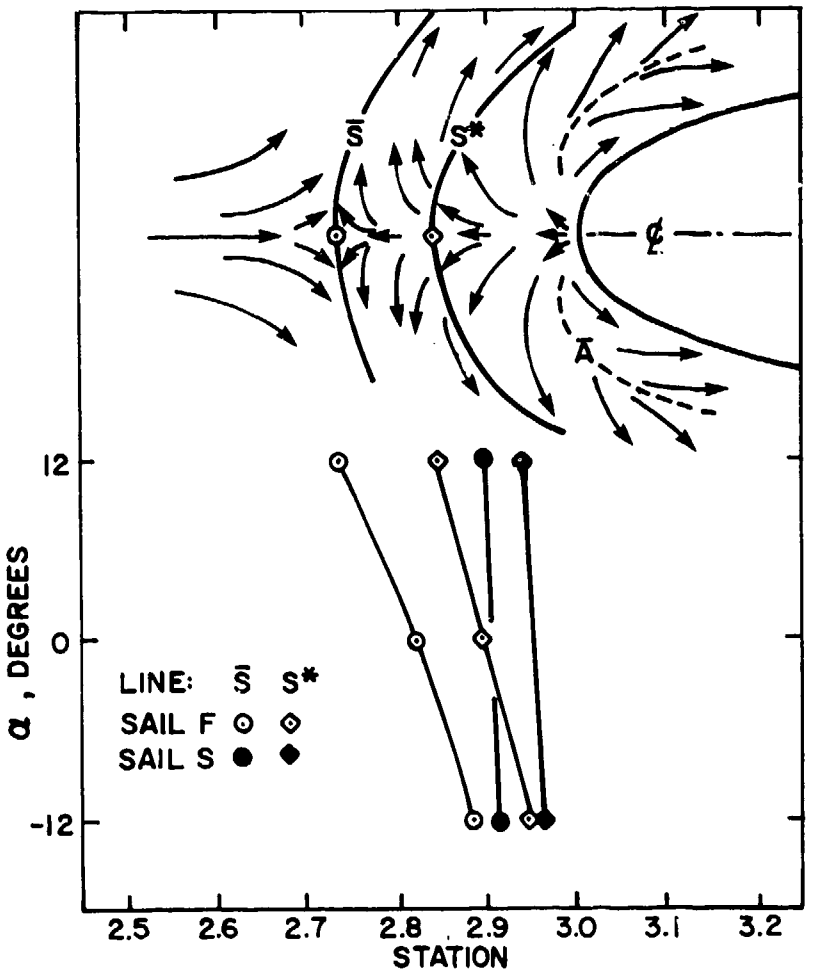

FIG. 34 SCHEMATIC LEADING EDGE JUNCTION FLOW AND ESTIMATES OF AXIAL LOCATION OF THE $\bar{S}$ AND S* LINES AS A FUNCTION OF PITCH

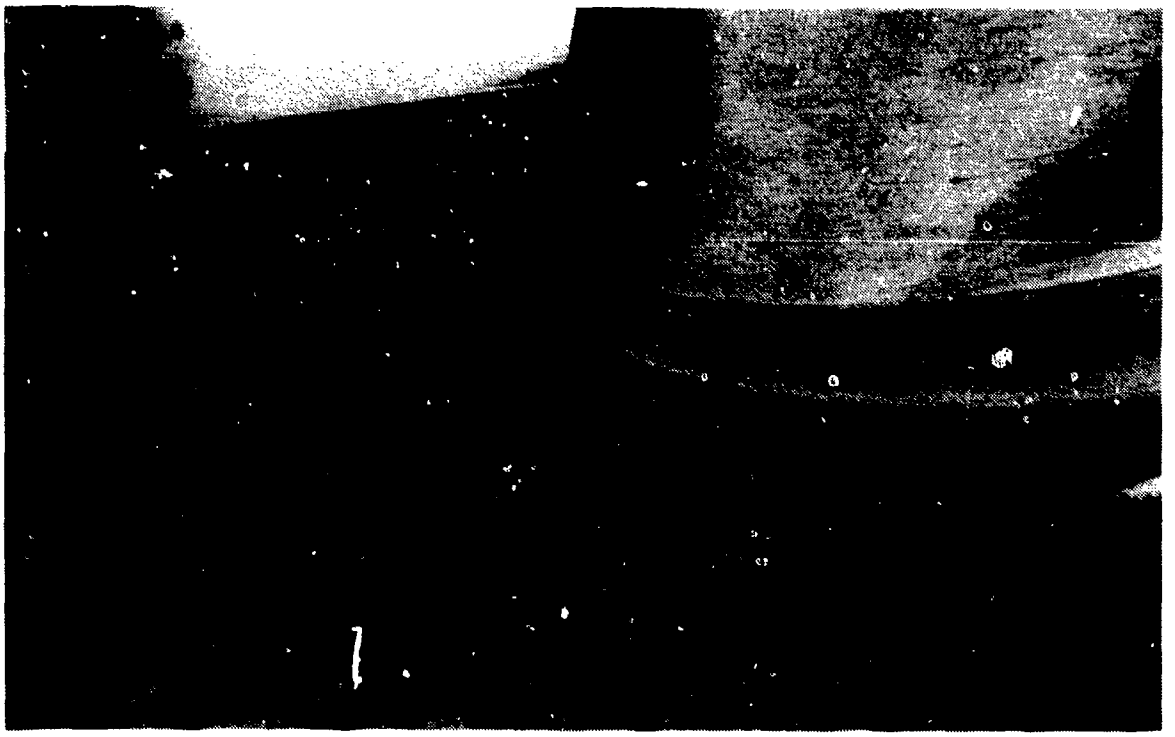

(a) β = 12 DEGREES

(b) β = 20 DEGREES

FIG. 35 SAIL S IN YAW : SAIL JUNCTION FLOW

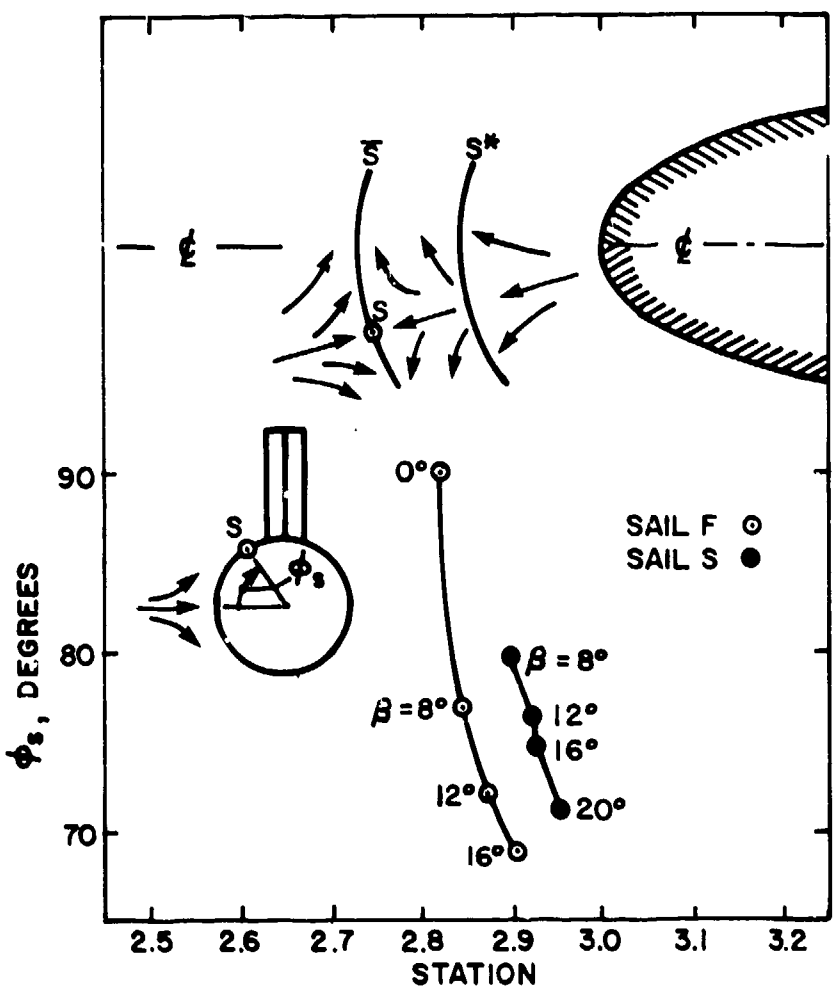

FIG. 36 SCHEMATIC LEADING EDGE JUNCTION FLOW AND ESTIMATES OF THE COORDINATES OF THE SADDLE POINT S AS A FUNCTION OF YAW

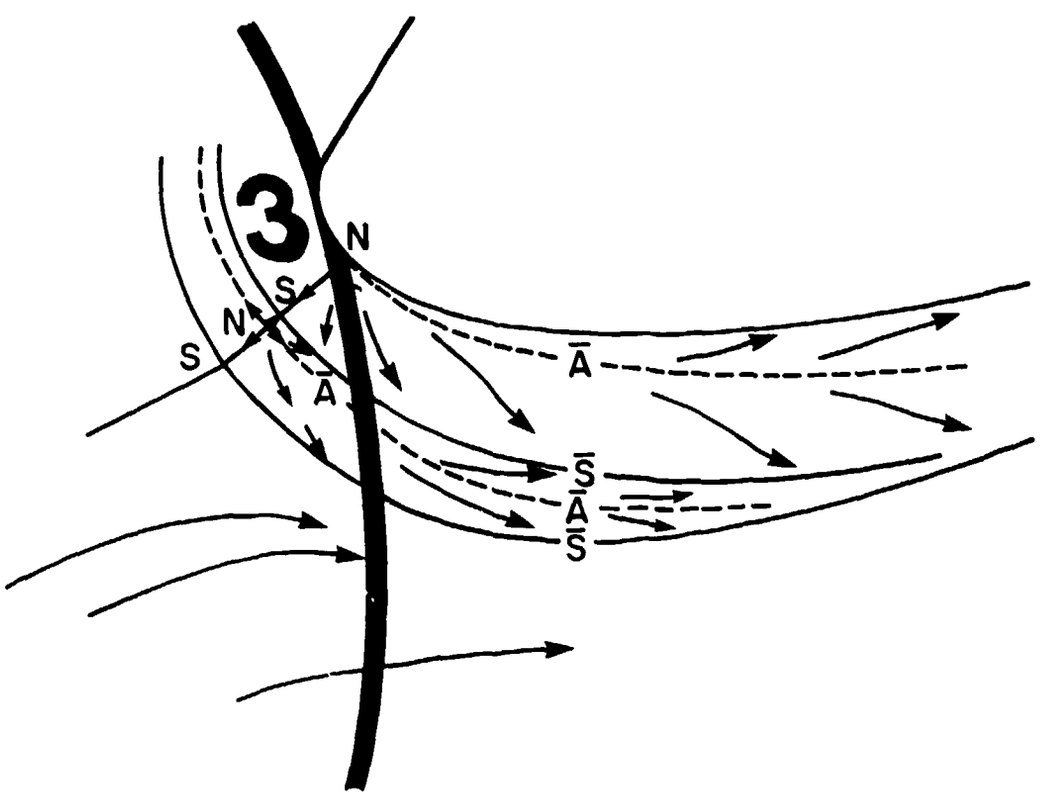

FIG. 37 SAIL S ON ASYMMETRIC HULL IN SIMULTANEOUS YAW AND PITCH ($\alpha = \beta = 8.55°$) : JUNCTION FLOW

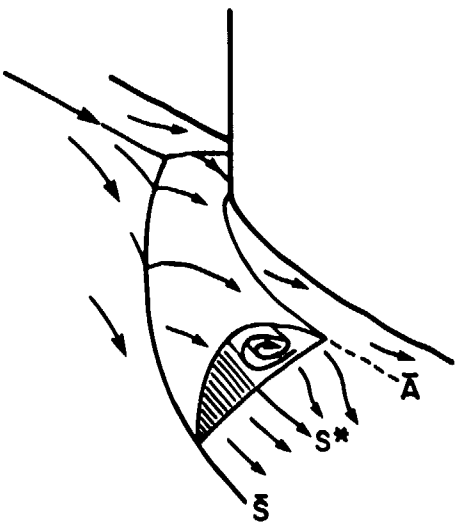

(a) WITHOUT SECONDARY SEPARATION

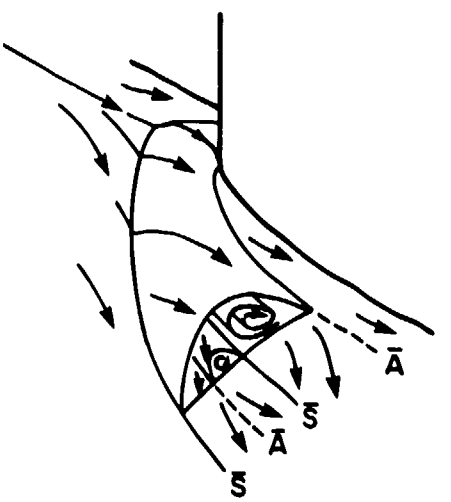

(b) WITH SECONDARY SEPARATION

FIG. 38 SAIL/HULL JUNCTION FLOW

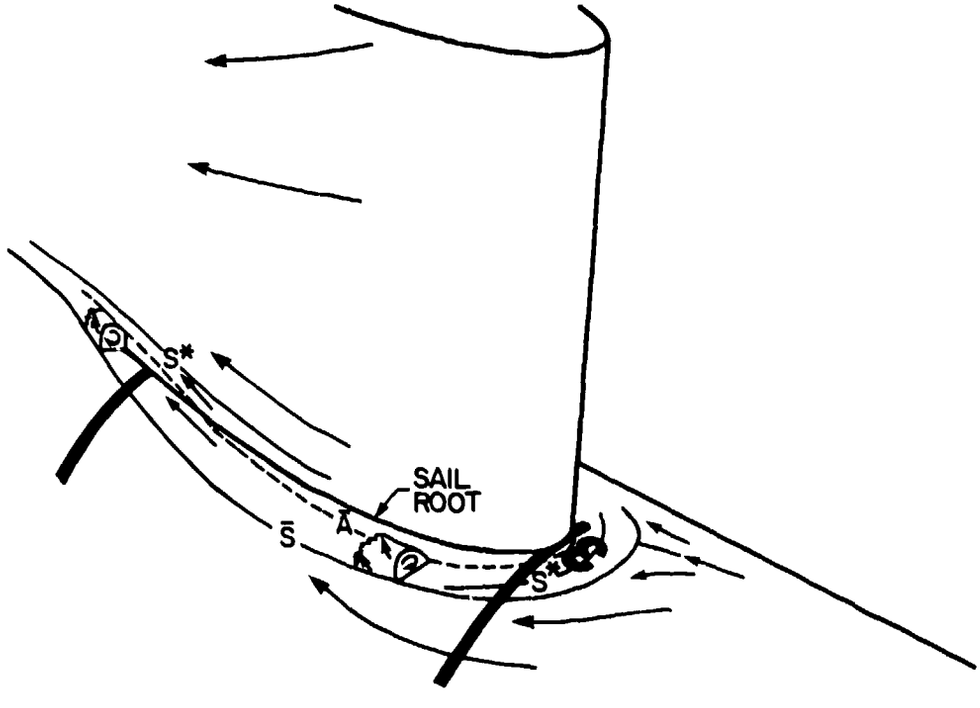

FIG. 39 SAIL S (ON AXISYMMETRIC HULL) AT 8° YAW : LEEWARD SIDE

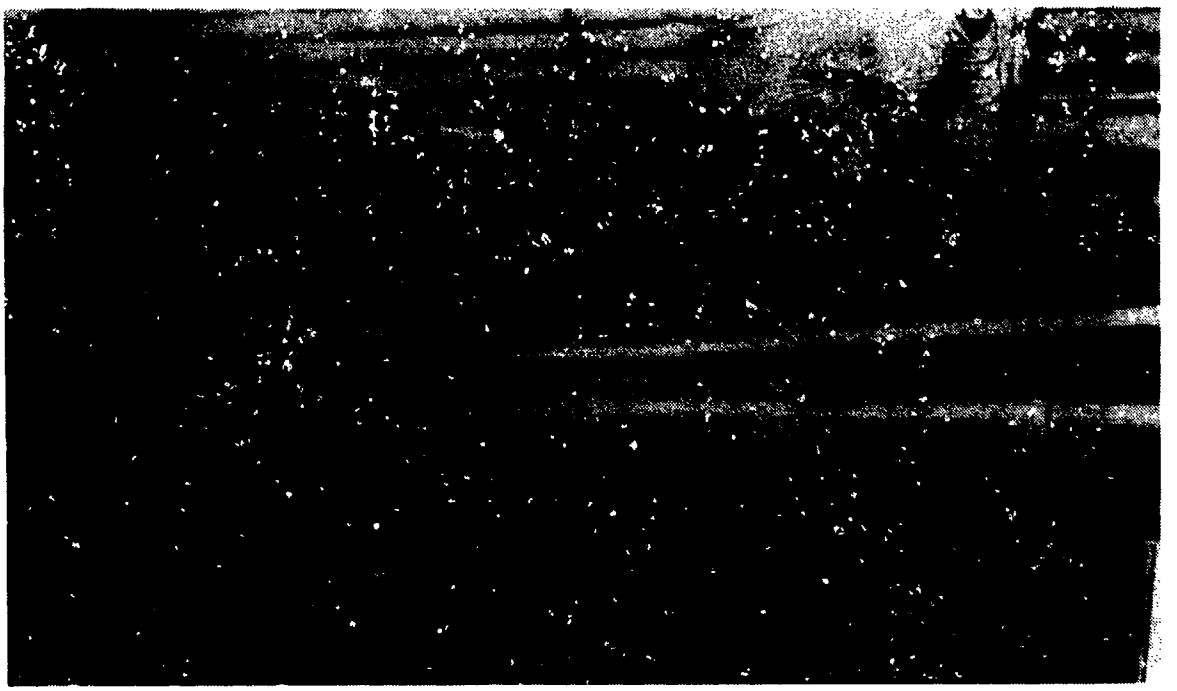

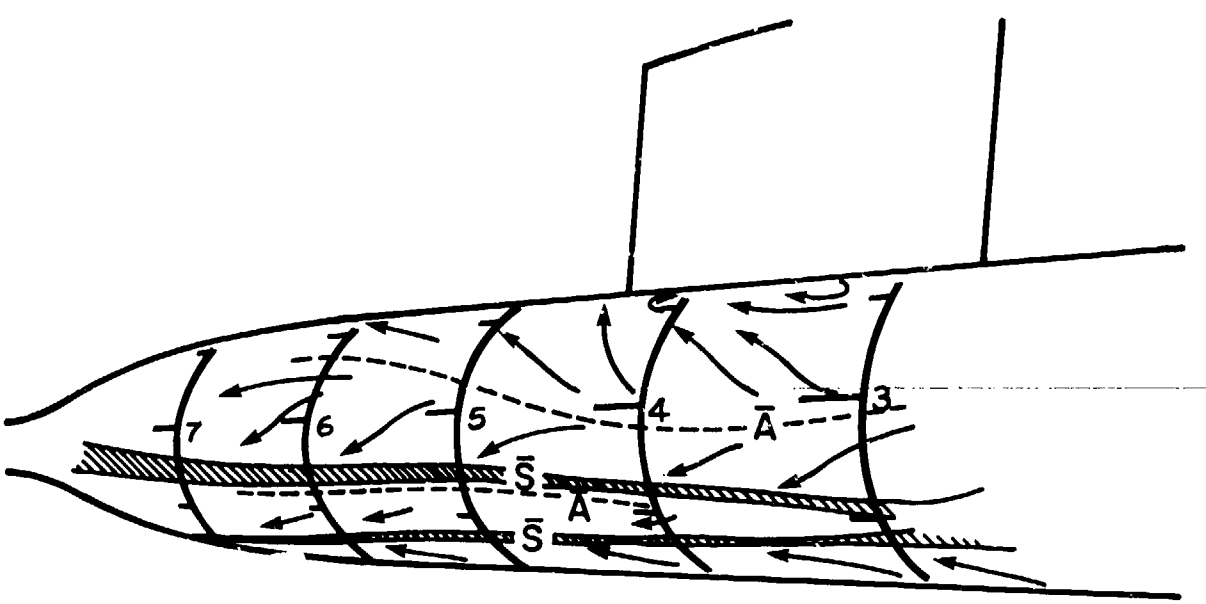

FIG. 40 HULL SEPARATION, SAIL S ON ASYMMETRIC BODY AT 20° YAW

REFERENCES

1. Mackay, M.: "Flow Visualization Experiments with Submarine Models in a Water Tunnel", DREA Technical Memorandum 86/220, September 1986.

2. Wardlaw, R.L.: "The National Aeronautical Establishment's 6 ft x 9 ft Low Speed Wind Tunnel", in: National Research Council of Canada DME/NAE Quarterly Bulletin No. 1962 (1), reprinted April 1962.

3. Riegels, F.W.: Aerofoil Sections, Butterworths, London, 1961.

4. Wickens, R.H.: "Observations of the Viscous Three-Dimensional Separations on Unpowered High-Wing Propeller Turbine Nacelle Models", NAE Laboratory Report LTR-LA-258, February 1982, INTERNAL DISTRIBUTION.

5. Squire, L.C., Maltby, R.L., Keating, R.F.A. and Stanbrook, A.: "The Surface Oil Flow Technique", in: "Flow Visualization in Wind Tunnels using Indicators" (Maltby, R.L., editor), AGARDograph 70, April 1962.

6. Oswatitsch, K.: "Die Ablosungsbedingung von Grenzschichten", IUTAM Symposium on Boundary-Layer Research, Freiburg, 1957.

7. Peake, D.J. and Tobak, M.: "Three-Dimensional Interactions and Vortical Flows with emphasis on High Speeds", AGARDograph No. 252, July 1980.

8. Hunt, J.C.R., Abell, C.J., Peterka, J.A. and Woo, H.: "Kinematical Studies of the Flows around Free or Surface-Mounted Obstacles; Applying Topology to Flow Visualization", J. Fluid Mech., Vol. 86 Part 1, pp. 179-200, 1978.

9. Meier, H.U., Kreplin, H.P. and Vollmers, H.: "Development of Boundary Layers and Separation Patterns on a Body of Revolution at Incidence", Second Symposium on Numerical and Physical Aspects of Aerodynamic Flows, CSU Long Beach, January 1983.

10. Dickinson, S.C.: "Flow Visualization and Velocity Measurements in the Separated Region of an Appendage-Flat Plate Junction", DTNSRDC SPD Report 86/020, March 1986.

11. Truckenbrodt, E.: "A Method of Quadrature for Calculation of the Laminar and Turbulent Boundary Layer in case of Plane and Rotationally Symmetric Flow (Translation)", NACA Technical Memorandum 1379, 1955.

12. Spangler, S.B., Sacks, A.H. and Nielsen, J.N.: "The Effect of Flow Separation from the Hull on the Stability of a High-Speed Submarine: Part I - Theory", Vidya Report No. 107, August 1963.

DOCUMENT CONTROL DATA

(Security classification of title, body of abstract and indexing annotation must be entered when the overall document is classified)

1. ORIGINATOR (the name and address of the organization preparing the document. Organizations for whom the document was prepared, e.g. Establishment sponsoring a contractor's report, or tasking agency, are entered in section 8.)

Defence Research Establishment Atlantic

2. SECURITY CLASSIFICATION (overall security classification of the document, including special warning terms if applicable)

Unclassified

3. TITLE (the complete document title as indicated on the title page. Its classification should be indicated by the appropriate abbreviation (S,C,R or U) in parentheses after the title.)

FLOW VISUALIZATION EXPERIMENTS WITH SUBMARINE MODELS IN A WIND TUNNEL

4. AUTHORS (Last name, first name, middle initial. If military, show rank, e.g. Doe, Maj. John E.)

Mackay, Michael

5. DATE OF PUBLICATION (month and year of publication of document)

January 1988

6a. NO. OF PAGES (total containing information. Include Annexes, Appendices, etc.)

57

6b. NO. OF REFS (total cited in document)

12

6. DESCRIPTIVE NOTES (the category of the document, e.g. technical report, technical note or memorandum. If appropriate, enter the type of report, e.g. interim, progress, summary, annual or final. Give the inclusive dates when a specific reporting period is covered.)

DREA Technical Memorandum

8. SPONSORING ACTIVITY (the name of the department project office or laboratory sponsoring the research and development. Include the address.)

9a. PROJECT OR GRANT NO. (if appropriate, the applicable research and development project or grant number under which the document was written. Please specify whether project or grant)

1AE

9b. CONTRACT NO. (if appropriate, the applicable number under which the document was written)

10a. ORIGINATOR'S DOCUMENT NUMBER (the official document number by which the document is identified by the originating activity. This number must be unique to this document.)

DREA TECH MEMORANDUM 88/204

10b. OTHER DOCUMENT NOS. (Any other numbers which may be assigned this document either by the originator or by the sponsor)

11. DOCUMENT AVAILABILITY (any limitations on further dissemination of the document, other than those imposed by security classification)

(X) Unlimited distribution
( ) Distribution limited to defence departments and defence contractors; further distribution only as approved
( ) Distribution limited to defence departments and Canadian defence contractors; further distribution only as approved
( ) Distribution limited to government departments and agencies; further distribution only as approved
( ) Distribution limited to defence departments; further distribution only as approved
( ) Other (please specify):

Unlimited

12. DOCUMENT ANNOUNCEMENT (any limitation to the bibliographic announcement of this document. This will normally correspond to the Document Availabilty (11). However, where further distribution (beyond the audience specified in 11) is possible, a wider announcement audience may be selected.)

Unclassified

SECURITY CLASSIFICATION OF FORM

13. ABSTRACT (a brief and factual summary of the document. It may also appear elsewhere in the body of the document itself. It is highly desirable that the abstract of classified documents be unclassified. Each paragraph of the abstract shall begin with an indication of the security classification of the information in the paragraph (unless the document itself is unclassified) represented as (S), (C), (R), or (U). It is not necessary to include here abstracts in both offical languages unless the text is bilingual).

Flow visualization experiments were carried out in the NAE 2 x 3 m low speed wind tunnel with some members of a systematic series of idealized submarine configurations. Only hull-alone and hull and sail configurations were tested. The experiments were done at Reynolds numbers between 4.9 and 9.5 million.

Results are reported for hull flow separation, flow on the sail and for flow in the sail/hull junction. In addition to some derived quantitative data, many photographs and interpretive sketches are included.

14. KEYWORDS, DESCRIPTORS or IDENTIFIERS (technically meaningful terms or short phrases that characterize a document and could be helpful in cataloguing the document. They should be selected so that no security classification is required. Identifiers, such as equipment model designation, trade name, military project code name, geographic location may also be included. If possible keywords should be selected from a published thesaurus. e.g. Thesaurus of Engineering and Scientific Terms (TEST) and that thesaurus-identified. If it is not possible to select indexing terms which are Unclassified, the classification of each should be indicated as with the title.)

Submarines
Wind Tunnel Testing
Flow Visualization

Unclassified

SECURITY CLASSIFICATION OF FORM